C/325

ANL-6174

MASTER

Argonne National Laboratory

# THE REACTOR KINETICS OF THE TRANSIENT REACTOR TEST FACILITY (TREAT)

by

D. Okrent, C. E. Dickerman,
J. Gasidlo, D. M. O'Shea,
and D. F. Schoeberle

## DISCLAIMER

**This report was prepared as an account of work sponsored by an agency of the United States Government. Neither the United States Government nor any agency Thereof, nor any of their employees, makes any warranty, express or implied, or assumes any legal liability or responsibility for the accuracy, completeness, or usefulness of any information, apparatus, product, or process disclosed, or represents that its use would not infringe privately owned rights. Reference herein to any specific commercial product, process, or service by trade name, trademark, manufacturer, or otherwise does not necessarily constitute or imply its endorsement, recommendation, or favoring by the United States Government or any agency thereof. The views and opinions of authors expressed herein do not necessarily state or reflect those of the United States Government or any agency thereof.**

**DISCLAIMER**

**Portions of this document may be illegible in electronic image products. Images are produced from the best available original document.**

*LEGAL NOTICE*

*This report was prepared as an account of Government sponsored work. Neither the United States, nor the Commission, nor any person acting on behalf of the Commission:*

*A. Makes any warranty or representation, expressed or implied, with respect to the accuracy, completeness, or usefulness of the information contained in this report, or that the use of any information, apparatus, method, or process disclosed in this report may not infringe privately owned rights; or*

*B. Assumes any liabilities with respect to the use of, or for damages resulting from the use of any information, apparatus, method, or process disclosed in this report.*

*As used in the above, "person acting on behalf of the Commission" includes any employee or contractor of the Commission, or employee of such contractor, to the extent that such employee or contractor of the Commission, or employee of such contractor prepares, disseminates, or provides access to, any information pursuant to his employment or contract with the Commission, or his employment with such contractor.*

*Price* $1.50 . *Available from the Office of Technical Services, Department of Commerce, Washington 25, D.C.*

ANL-6174
Reactors - General
(TID-4500, 15th Ed.)
AEC Research and
Development Report

ARGONNE NATIONAL LABORATORY
9700 South Cass Avenue
Argonne, Illinois

# THE REACTOR KINETICS OF THE TRANSIENT REACTOR TEST FACILITY (TREAT)

by

D. Okrent, C. E. Dickerman, J. Gasidlo,
D. M. O'Shea, and D. F. Schoeberle

Reactor Engineering Division

September, 1960

Operated by The University of Chicago
under
Contract W-31-109-eng-38

# TABLE OF CONTENTS


| | Page |
|---|---|
| INTRODUCTION | 7 |
| I. STATIC CHARACTERISTICS | 9 |
| A. Description of Reactor | 9 |
| B. Methods of Calculation Used | 19 |
| C. Criticality Calculations | 22 |
| D. Neutron Energy Spectrum | 25 |
| E. Prompt Neutron Lifetime | 31 |
| F. Temperature Coefficients | 32 |
| II. ANALYSIS OF TREAT TRANSIENTS | 35 |
| A. Introduction | 35 |
| B. Experimental Data Reduction | 35 |
| 1. Use of Data | 35 |
| 2. Calculation of $k_{eff}$ | 38 |
| 3. Conversion of TREAT Power to Neutron Density | 44 |
| C. Theoretical Calculations of Feedback | 44 |
| 1. Reactor Temperature as a Function of $\int n\,dt$ | 44 |
| 2. Calculation of $k_{ex}$ as a Function of $\int n\,dt$ | 47 |
| D. Fit to Experimental Data | 47 |
| 1. Techniques | 47 |
| a. Theoretical Neutron Density Calculations | 47 |
| b. Absolute Normalization of Theoretical Calculations | 48 |
| c. Check of Feedback Curve Shape | 51 |
| 2. Results of Comparisons | 52 |
| a. Direct Comparison of Calculated and Experimental Feedback | 52 |
| b. Power Curve Shape | 53 |
| c. Maximum Transient Power Values | 56 |
| d. Integrated Power Values | 56 |
| e. Maximum Reactor Temperatures | 59 |
| E. Performance Extrapolations | 60 |
| REFERENCES | 64 |

# LIST OF TABLES


| No. | Title | Page |
|---|---|---|
| I. | Volume Fractions for TREAT Cells | 16 |
| II. | Volume Fractions, by Element, in TREAT Materials | 17 |
| III. | Atomic Concentrations at Reference Density | 18 |
| IV. | Spherical Representation of TREAT with Average Composition Reflector | 18 |
| V. | Energy Breakdown of Twenty-group, Gas Model Cross Sections | 21 |
| VI. | Cadmium Ratios | 25 |
| VII. | Delayed-neutron Parameters Calculated for TREAT | 42 |
| VIII. | Normalization of Twenty-group Gas Model Calculations | 51 |

# LIST OF FIGURES


| No. | Title | Page |
|---|---|---|
| 1. | TREAT Reactor Perspective | 10 |
| 2. | TREAT Plan View | 11 |
| 3. | Standard TREAT Fuel Assembly | 12 |
| 4. | Types of TREAT Fuel Assemblies | 13 |
| 5. | TREAT Elevation View | 14 |
| 6. | TREAT Plan View (Dimensioned) | 15 |
| 7. | Multiplication Factor, $k_{eff}$, vs. Core Size | 23 |
| 8. | Radial $U^{235}$ Fission Rate in TREAT | 24 |
| 9. | Axial $U^{235}$ Fission Rate in TREAT | 24 |
| 10. | Neutron Energy Spectrum at Core Center | 28 |
| 11. | $Pu^{239}/U^{235}$ Fission Ratio vs. Moderator Temperature at Core Center | 29 |
| 12. | Axial Variation of $Pu^{239}/U^{235}$ Fission Ratio (Moderator Temperature 300°K) | 30 |
| 13. | Axial Variation of $Pu^{239}/U^{235}$ Fission Ratio for Non-Uniform Moderator Temperature | 30 |
| 14. | $k_{eff}$ vs. $\epsilon$, the Convergence Criterion, for the Fire Code | 32 |
| 15. | Twenty-group Gas Model Prediction of Temperature Coefficient of Reactivity vs. Core Moderator Temperature | 33 |
| 16. | Power Traces for 0.595% $k_{ex}$ Transient | 39 |
| 17. | Power Traces for 1.16% $k_{ex}$ Transient | 39 |
| 18. | $k_{ex}(t)$ Calculations from Power Traces of Figure 16 | 40 |
| 19. | $k_{ex}(t)$ Calculations from Power Traces of Figure 17 | 40 |
| 20. | Comparison of Initial $k_{ex}$ from Asymptotic Period with that from Rod Calibrations | 43 |
| 21. | Typical Core Temperature Traces from the 0.595% $k_{ex}$ and 0.87% $k_{ex}$ Transients | 45 |
| 22. | TREAT Fuel Enthalpy | 46 |
| 23. | TREAT Temperature-Integrated Neutron Density Relationship | 46 |
| 24. | Calculated $k_{ex}$-Integrated Neutron Density Relationship | 47 |
| 25. | Power Feedback Normalization Example | 50 |

# LIST OF FIGURES


| No. | Title | Page |
|---|---|---|
| 26. | Comparison of Calculated and Experimental $k_{ex}$-Integrated Neutron Density Data | 53 |
| 27. | Comparison of Calculated and Experimental Power Curve Shapes for 0.595% $k_{ex}$ Transient | 54 |
| 28. | Comparison of Calculated and Experimental Power Curve Shapes for 1.16% $k_{ex}$ Transient | 55 |
| 29. | Comparison of Calculated and Experimental Power Curve Shapes for 1.92% $k_{ex}$ Transient | 56 |
| 30. | Comparison of Calculated and Experimental Power Curve Shapes for the Transient Initiated at Elevated Temperature | 57 |
| 31. | Comparison of Calculated and Experimental Maximum Transient Power Data | 58 |
| 32. | Comparison of Calculated and Experimental Integrated Transient Power Data | 58 |
| 33. | Comparison of Calculated and Experimental Maximum Reactor Temperature Data | 60 |
| 34. | TREAT Extrapolated Normalized $k_{ex}$-Integrated Neutron Density Relationship | 61 |
| 35. | Transient Power Curves Calculated Using Extrapolated Normalized Feedback | 61 |
| 36. | Integrated Transient Power Values Calculated Using Extrapolated Normalized Feedback | 62 |
| 37. | Maximum Reactor Temperatures Calculated Using Extrapolated Normalized Feedback | 62 |
| 38. | Maximum Transient Power Values Calculated Using Extrapolated Normalized Feedback | 63 |

# THE REACTOR KINETICS OF THE TRANSIENT REACTOR TEST FACILITY (TREAT)

by

D. Okrent, C. E. Dickerman, J. Gasidlo,
D. M. O'Shea, and D. F. Schoeberle

## INTRODUCTION

The Transient Reactor Test Facility (TREAT) is a pulsed, graphite-moderated reactor constructed by Argonne National Laboratory at the National Reactor Testing Station especially to generate safely very large integrated bursts of thermal neutrons over a large sample volume. The reactor was inspired by the needs of the fast reactor safety program[1] for a facility in which the core meltdown problem could be studied in-pile. It was designed to enable a rapid heating leading to destruction of mockups of fast reactor fuel elements under controlled conditions, without harm to the reactor itself. A near maximization of available total neutrons was taken as the primary design goal, in order to provide the greatest possible flexibility in experimental techniques, such as the use of natural or low-enrichment fuel pins. As a consequence, in the original reference design, the core-averaged, time-integrated thermal flux of $\sim 3 \times 10^{15}$ nvt (which has been exceeded in actual performance) is an order of magnitude greater than that produced in the final destructive transient of BORAX I. This integrated flux is more than twice that required to melt a natural enrichment EBR-II fuel element.

To achieve this maximization of flux integral, a maximization of immediately available heat capacity per fissionable atom is required of the reactor. A uniform dispersion of uranium oxide within a graphite matrix was chosen, with all the graphite moderator in intimate contact with the fuel. The moderator then acts as a giant heat sink, absorbing the energy generated in the 20-micron sized uranium particles with time lags of the order of one millisecond, much more rapidly than coolant could carry it away. Furthermore, on heating, the graphite in turn raises the energy of the thermal neutrons and increases their probability of leaking, thereby generating a sizeable negative temperature coefficient.

In the case of self-limited bursts (transients terminated by the built-in temperature coefficient rather than by control rod action), the prompt neutron lifetime and temperature coefficient of reactivity play the major role in defining the sharpness of the burst available. However, the experimental demands of the fast reactor safety program do not impose a requirement of power pulses having a half-width of a few milliseconds, but rather define the interesting range of experiments as covering times of

power input ranging from hundreds of milliseconds to tens of seconds. A fifty-millisecond half-width is available with the existing design, and specially programmed control rods enable an extension of the burst width to tens of seconds at essentially constant power. Hence, in the design of the reactor, possible variations, such as reducing the thermal neutron return from the reflector, which could shorten the neutron lifetime, or the addition of non-1/v-absorbers, which could amplify the temperature coefficient, were not considered, since they would also reduce the available integrated flux.

The reactor was originally described by Freund, Iskenderian and Okrent at the Second Geneva Conference on Peaceful Uses of Atomic Energy.[2] Further details on its engineering features are given in a hazards summary report[3] and a design report.[4] Criticality calculations associated with the design of the reactor have also been reported,[5] as well as a modification of these predictions made on the discovery of some boron impurities in the core graphite.[6] Preliminary experimental results on the kinetic behavior of the reactor,[7] and theoretical interpretation thereof,[8] were reported at the November, 1959, meeting in Washington, D. C., of the American Nuclear Society.

The experimental reactor physics measurements pertinent to the TREAT reactor in its simplest form, i.e., a uniform cylindrical core without slots or test holes, will be published[9] as a companion report to this work, and the pair provide a fairly complete summary of the information available to date on the kinetic behavior of the reactor.

This report has been divided into two major sections as a matter of convenience. In the first section, the various static characteristics of the reactor which pertain to its dynamic behavior, such as temperature coefficient and prompt neutron lifetime, are discussed. Also considered in the first section are certain other phenomena, the analyses of which provide some measure of the general adequacy of the calculational techniques employed. The second section covers the correlation and analysis of the results of transient experiments on this clean geometry TREAT reactor in considerable detail. In addition, an extrapolation of its performance beyond the present low design limitation of 400C maximum local temperature is included in Section II.

# I. STATIC CHARACTERISTICS

## A. Description of Reactor

A general description of the reactor is given in Figs. 1 and 2. As can be seen, the reactor consists of a right cylindrical core, fully reflected by graphite. In its normal operation as a pulsed engineering test reactor, there is usually a vertical central hole containing the sample, and there may be one or more large slots running horizontally from the core center out through the reflector. The size of the core is adjusted to provide the necessary excess reactivity to run the various transients required for test operations.

To expedite analysis of the reactor behaviour, early reactor physics experimentation was performed on the simplest configuration possible within the framework of the reactor structure. An approximately round, right cylindrical core, of reasonably good homogeneity, was built with the smallest core radius compatible with the particular experiment in mind. Due to fuel element construction limitations, the core was always 120.97 cm high, with an aluminum-clad graphite reflector top and bottom. The radial reflector was composed of two parts. The adjustable inner reflector consisted of dummy fuel elements which replaced that portion of the core cavity not being used for fuel. This adjustable reflector used a ring of zirconium-clad dummy elements next to the core, and aluminum-clad elements for the remainder. A permanent reflector, of slightly different composition, was constructed beyond the core cavity.

The design of typical fuel elements, control rod elements and reflector elements, including dimensions, is given in Figs. 3 and 4, while the dimensions of the various regions of the core and reflectors are presented in Figs. 5 and 6.

Volume fractions have been derived separately for each possible TREAT region, on the assumption that each region is to be composed of one or several types of elements as appropriate. The volume fractions for individual types of elements are given in Table I. Each of these elements can be further subdivided into three separate cells (core, upper reflector, and lower reflector) in addition to a further allowance for an "axial interface" cell which is discussed separately. Each type of cell will be identified hereafter by the letter accorded it in Table I.

The axial interface cells (at the core-upper reflector and core-lower reflector interfaces) were added late in the TREAT design. Each cell contains a 0.396-cm thick Zircaloy plate and a 0.635-cm ribbed Zircaloy spacer. These regions were added to form a heat barrier insulating the less heat-resistant aluminum-clad reflector cells from the core. These cells will occur above and below the types A, B, and D cells of Table I.

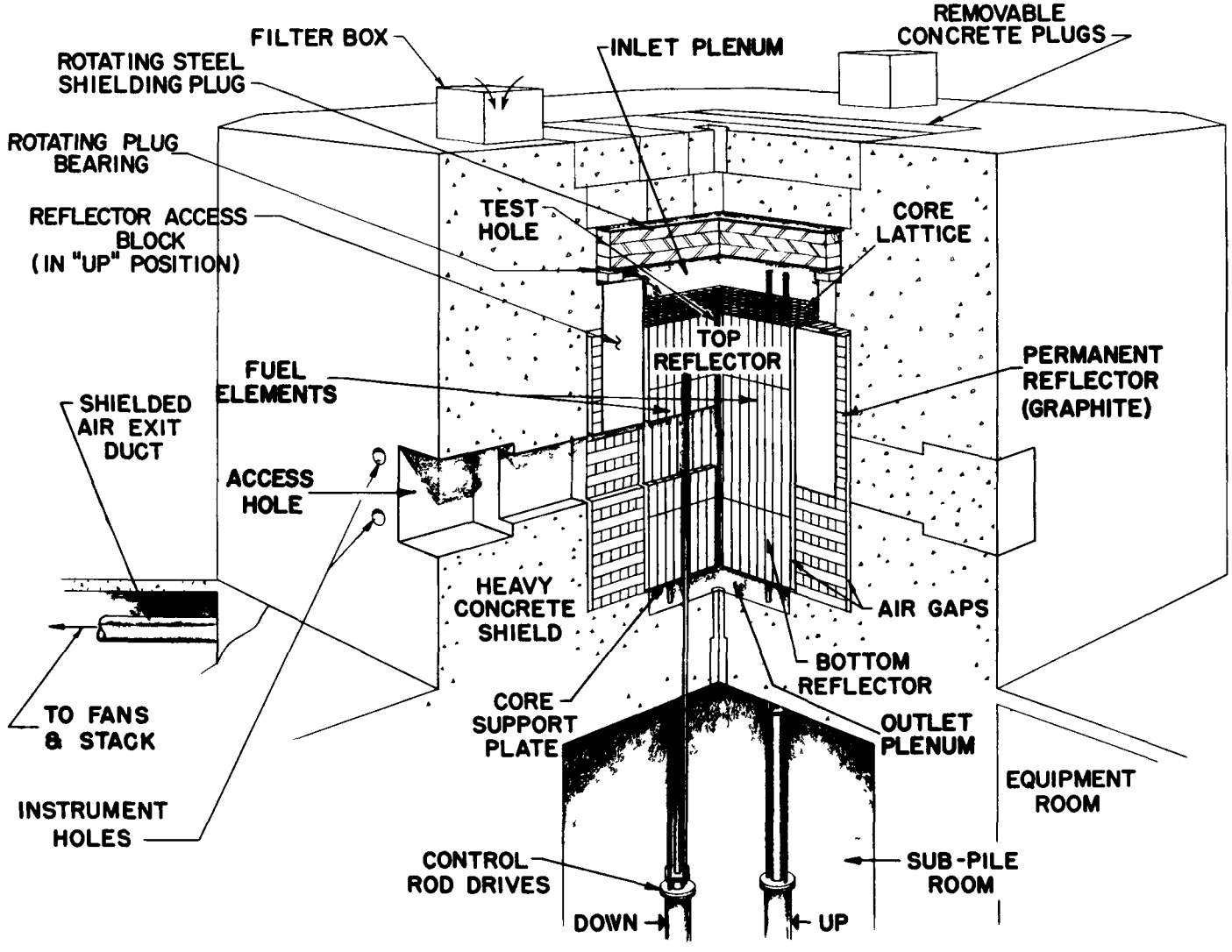


FIG. 1
TREAT REACTOR PERSPECTIVE

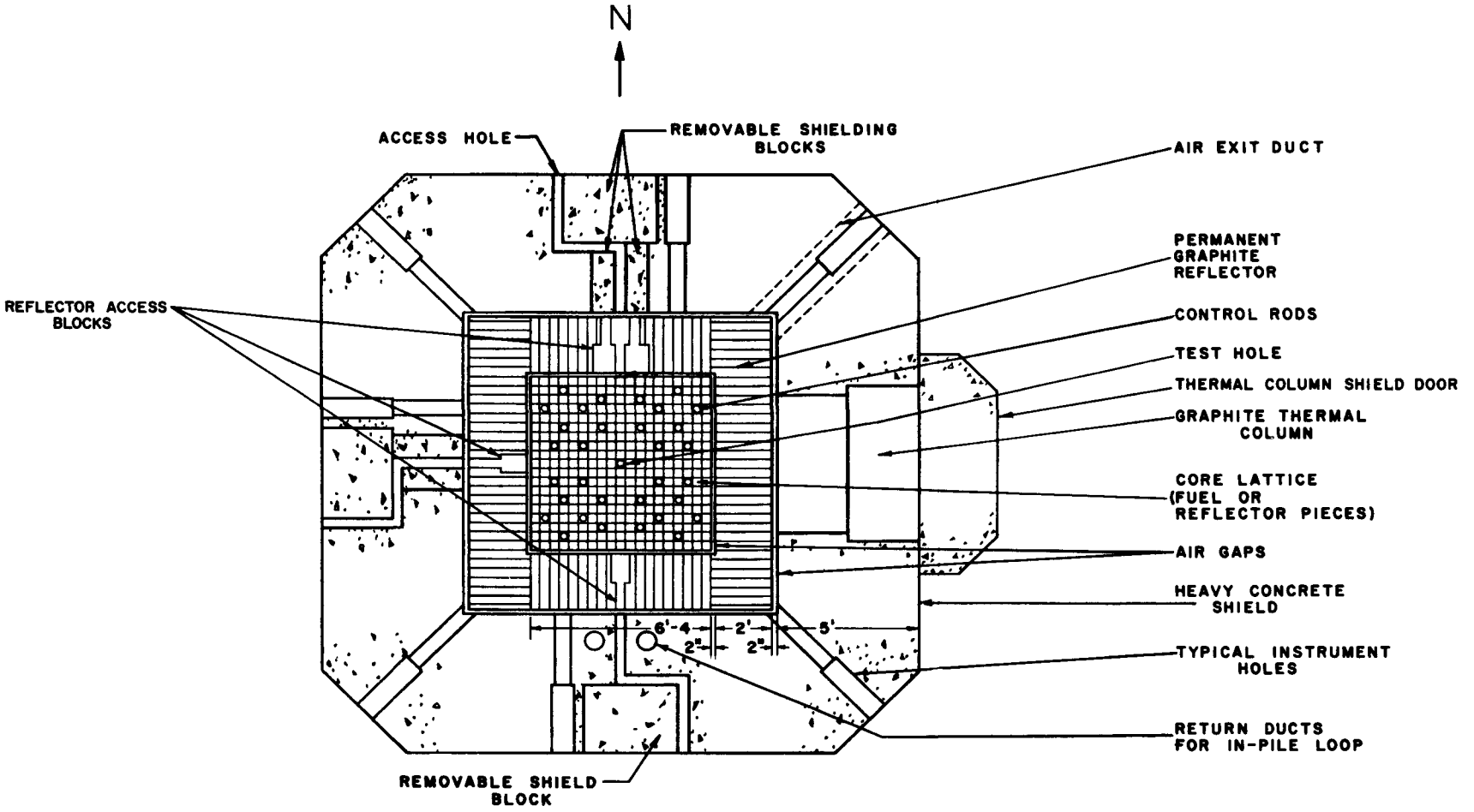


FIG. 2
TREAT PLAN VIEW

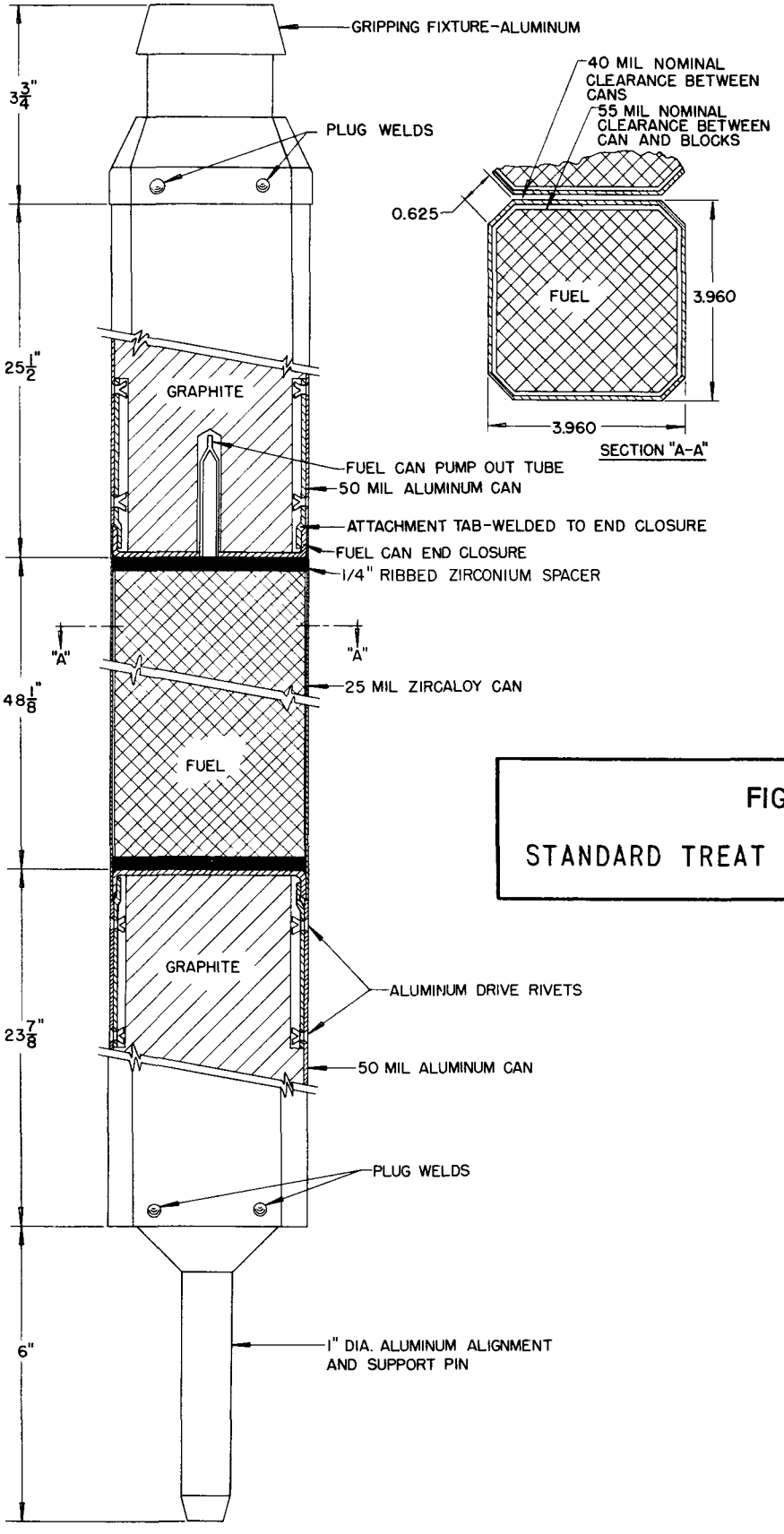


FIG. 3

STANDARD TREAT FUEL ASSEMBLY

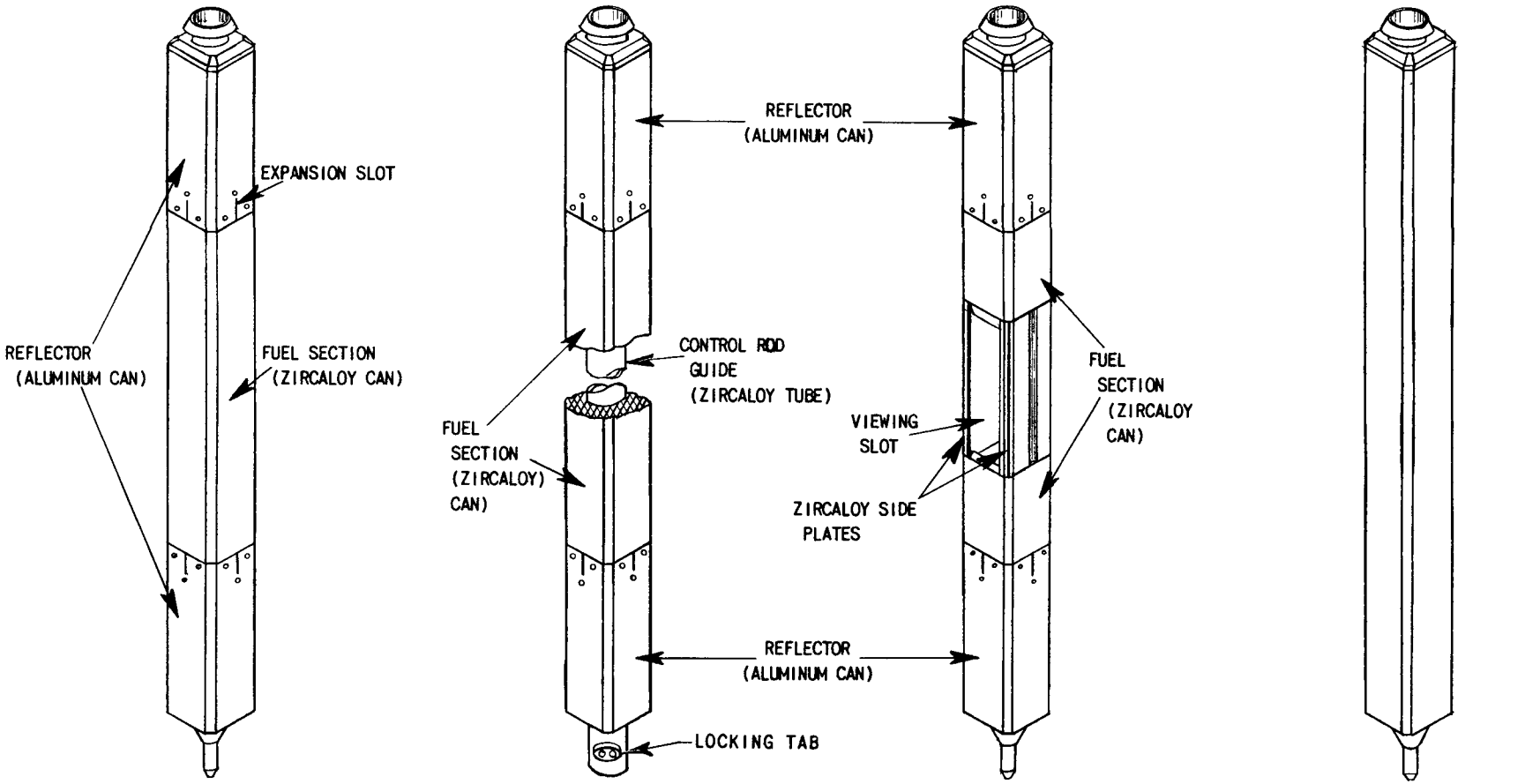


FIG. 4
TYPES OF TREAT FUEL ASSEMBLIES

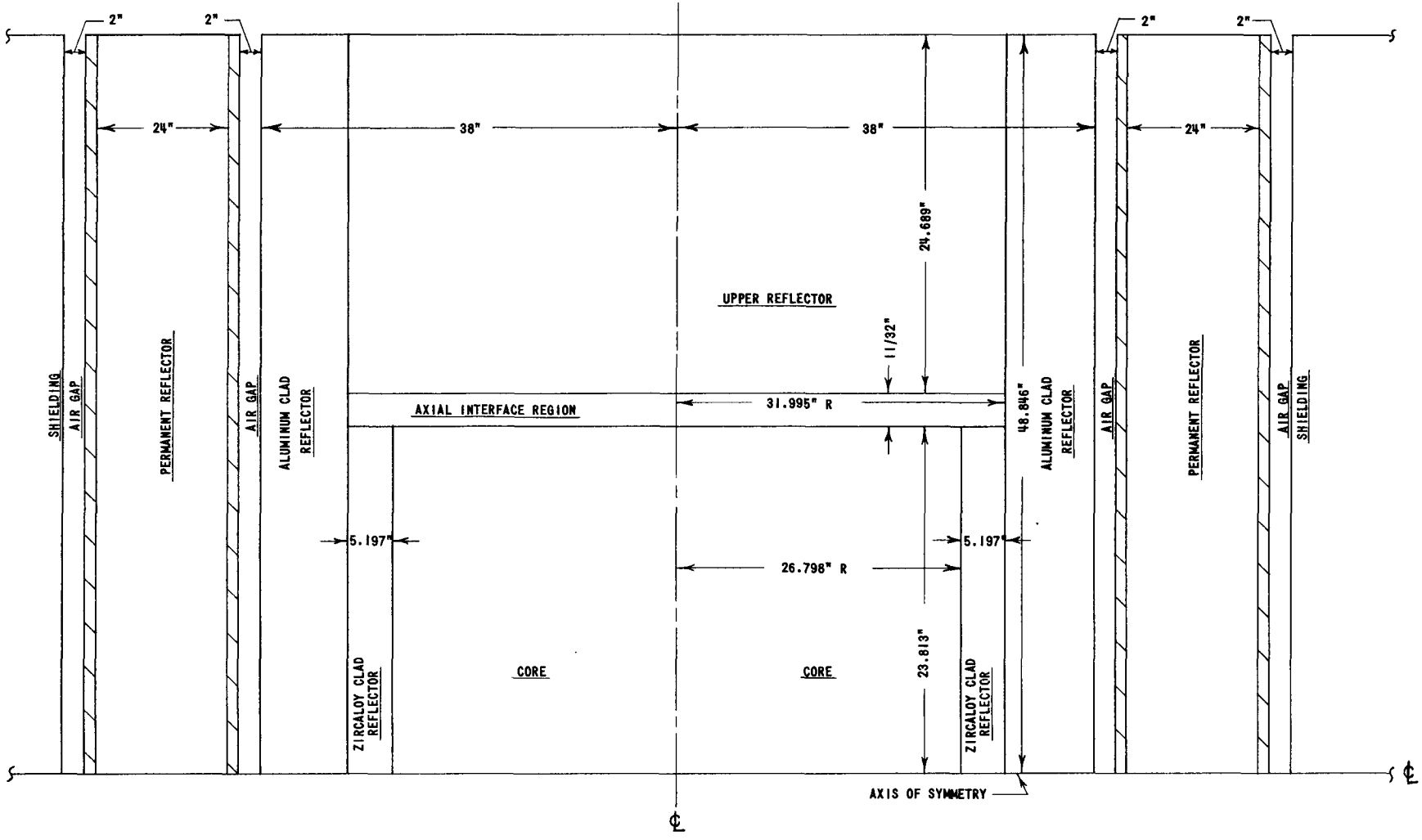


FIG. 5
TREAT ELEVATION VIEW (SECTION "AA")
NOT TO SCALE
(CONTROL ROD ELEMENTS NOT SHOWN)

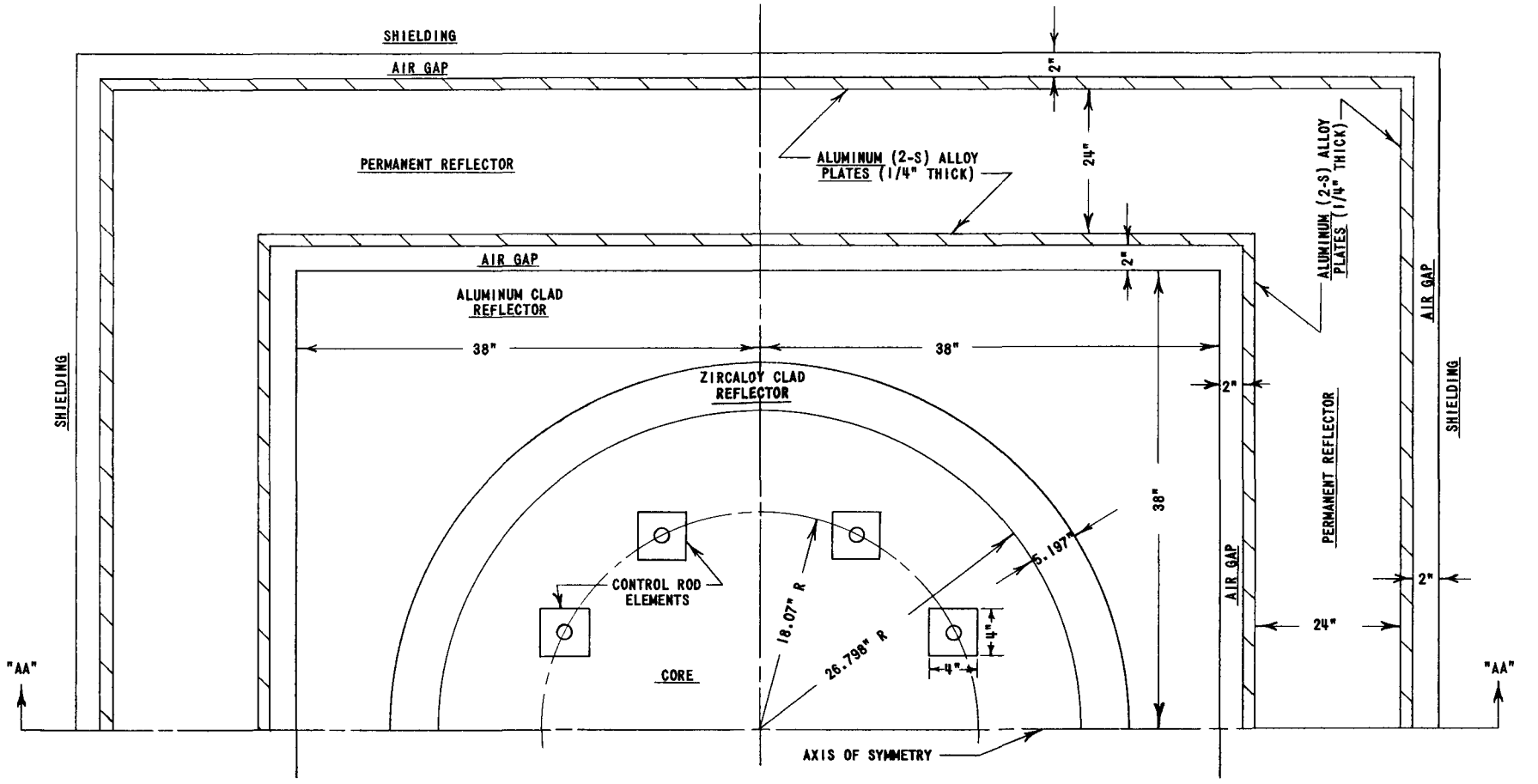


FIG. 6
TREAT PLAN VIEW (DIMENSIONED)
(NOT TO SCALE)

Table I

VOLUME FRACTIONS FOR TREAT CELLS

| Type | | | | | | | | Material Description |
|---|---|---|---|---|---|---|---|---|
| A<br>Normal Core Fuel Cells | B<br>Control Rod Fuel Cells | C<br>Normal Al-clad Reflector Cells | D<br>Dummy Zircaloy-clad Reflector Cells | E<br>Upper Reflector Control Rod Cells | F<br>Lower Reflector Control Rod Cells | G<br>Axial Interface Cells | H<br>Permanent Reflector | |
| 0.8905 | 0.6241 | | | | | | | Core Graphite |
| | 0.1105 | 0 8701 | 0.8905 | 0.6539 | 0 7141 | | 0.9057 | Reflector Graphite |
| 0 0231 | 0 0231 | | 0 0231 | | | 0 3258 | | Zircaloy-3-clad |
| | 0.0921 | | | 0 0398 | 0 0920 | | | Zircaloy-2 (in tubes) |
| | | 0.0463 | | 0 1567 | 0.0463 | | | Aluminum (6063-S) Alloy Clad |
| | | | | | | | 0.0189 | Aluminum 2-S Alloy |
| 0.0864 | 0.1502 | 0.0836 | 0.0864 | 0.1496 | 0 1476 | 0 6742 | 0 0754 | Void |

Throughout this study, the two air gaps and two aluminum alloy plates surrounding the stacked graphite of the permanent reflector were assumed to be part of the permanent reflector. Cell type "H" includes this preliminary homogenization.

The materials given in Table I were next separated into their constituents, by means of the known chemical compositions. The aluminum 2-S alloy was assumed to contain impurities represented by 1.0 wt-% iron, and thus 99 wt-% aluminum is the remainder. The aluminum 6063-S alloy contains 98.5 wt-% aluminum and 1.5 wt-% of impurities, again assumed to be represented by iron.

The Zircaloy-2 and Zircaloy-3 alloys are known to contain about 99.52 wt-% zirconium , 0.24 wt-% iron, and 0.24 wt-% tin, with only negligible traces of other elements. Although the Zircaloy-2 does contain slightly more impurities, the difference between the two alloys was neglected because extremely small amounts of Zircaloy-2 are present in TREAT.

The "reflector graphite" used throughout TREAT was reclaimed from the dismantled CP-2 reactor. This graphite has density $d^C$ = 1.67 gms/cc, and impurities represented, in the present study, by 2.0 ppm boron and 1,000 ppm iron. These figures represent the upper limits of the results of spectrochemical analyses made on samples of this graphite, which are presented as Table VII of Reference 6.

The core graphite, used only in normal core fuel cells and control rod fuel cells, was prepared especially for TREAT. This graphite is a homogeneous mixture of uranium carbide, normal graphite, and impurities, and it has density $d^C$ = 1.72 gms/cc. The final uranium content was determined by sampling techniques and gave a mean value of 0.2109 wt-% uranium.[10] The impurities in this graphite were again determined by spectrochemical analyses of many samples. Because the boron impurity content of this graphite varied greatly from sample to sample, a set of reference impurities of 6.0 ppm boron and 1,000 ppm iron was chosen at the beginning of the present study and maintained throughout.[6] The uranium loaded into the graphite was 93.1 wt-% $U^{235}$.

Using the above given concentrations of impurities, uranium, etc., the concentration by volume of each element in each reactor material was derived and is presented in Table II.

Table II

VOLUME FRACTIONS, BY ELEMENT, IN TREAT MATERIALS

| Element | Material | | | | |
|---|---|---|---|---|---|
| | Core Graphite | Reflector Graphite | Zircaloy | Al 6063-S Alloy | Al 2-S Alloy |
| Carbon I | 0.999585 | | | | |
| Boron | $4.21 \times 10^{-6}$ | $1.36 \times 10^{-6}$ | | | |
| Iron | $2.188 \times 10^{-4}$ | $2.125 \times 10^{-4}$ | $2.0041 \times 10^{-3}$ | 0.005172 | $3.4478 \times 10^{-3}$ |
| $U^{235}$ | $1.787 \times 10^{-4}$ | | | | |
| $U^{238}$ | $1.32 \times 10^{-5}$ | | | | |
| Tin | | | $2.3544 \times 10^{-3}$ | | |
| Zirconium | | | 0.995642 | | |
| Aluminum | | | | 0.994828 | 0.996552 |
| Carbon II | | 0.999786 | | | |

Table III presents the atomic concentration of each element, at reference density, for use in connection with Table II. The product of volume fraction of the element (from Table II) and the density factor (from Table III) gives the usual atomic density of each element in a particular material.

Table III

ATOMIC CONCENTRATIONS AT REFERENCE DENSITY

| Material i | Reference Density, $\rho_i$ (gm/cc) | $N = (N_0\rho/A) \times 10^{-24}$ |
|---|---|---|
| Carbon I | 1.72 | 0.086275 |
| Boron | 2.45 | 0.136419 |
| Iron | 7.86 | 0.084788 |
| $U^{235}$ | 18.90 | 0.048428 |
| $U^{238}$ | 18.90 | 0.047827 |
| Tin | 6.50 | 0.032991 |
| Zirconium | 6.40 | 0.042269 |
| Aluminum | 2.699 | 0.060269 |
| Carbon II | 1.67 | 0.083767 |

The compositions and geometry to be used in a specific calculation can be assigned from a knowledge of the actual configuration, the data in Tables II and III, and the limitations imposed by the computation methods. For many calculations, spherical geometry is convenient; a spherical approximation of the reactor, with an "average" reflector, is presented in Table IV.

Table IV

SPHERICAL REPRESENTATION OF TREAT WITH AVERAGE COMPOSITION REFLECTOR

| $N \times 10^{-24}$ atoms/cc | | |
|---|---|---|
| Element | 141-element Core | Average Reflector |
| $U^{235}$ | $7.5742 \times 10^{-6}$ | |
| $U^{238}$ | $5.5431 \times 10^{-7}$ | |
| Zirconium | $1.1903 \times 10^{-3}$ | $1.9533 \times 10^{-4}$ |
| Boron | $5.047 \times 10^{-7}$ | $1.5961 \times 10^{-7}$ |
| Iron | $3.3435 \times 10^{-5}$ | $7.8934 \times 10^{-5}$ |
| Aluminum | | $2.605 \times 10^{-3}$ |
| Carbon | 0.0760275 | 0.072216 |
| Radii - Sphere | | |
| Core 71 cm | | Average Reflector 166.7 cm |

B. Methods of Calculation Used

A variety of calculation methods have been used to study various aspects of the static performance of TREAT. They are outlined below:

(1) A three-group diffusion theory calculation, similar to that adopted by Iskenderian in ANL-6025.[5] The fast group terminated at 1.44 ev, and the epithermal at 0.4 ev. There was no scattering upward in energy from group 3 to group 2.

The treatment of the Fermi ages and reactor ages followed that of ANL-6025[5] exactly. The Fermi age in graphite is assumed to consist of two components, one above and one below the indium resonance energy E = 1.44 ev. The Fermi age above E = 1.44 ev is taken from the experimental value[11] of 271.8 $cm^2$ for graphite of density $\rho$ = 1.71 $gms/cm^3$. The Fermi age contribution below E = 1.44 ev is calculated from the integral

$$\Delta\tau^F = \int_{E_{eff}}^{1.44\ ev} \frac{dE/E}{3\xi(E)\Sigma_s \Sigma_{TR}} \quad , \tag{1}$$

where

$$\xi(E) = \frac{2}{m}\left[1 - \frac{2kT_0}{E} + \frac{\Delta}{4}\left(\frac{kT_0}{E}\right)^{3/2}\right] \quad , \tag{2}$$

with

$E_{eff} = 2E_n$

$E_n$ = Peak energy of thermal energy spectrum

$T_0$ = Moderator temperature

$\Delta$ = The absorption parameter = $2m\alpha$ (see Reference 12)

$m$ = Mass of carbon atom/mass of a neutron.

$\Sigma_s, \Sigma_{TR}$ = Scattering and transport cross sections, respectively, at the desired graphite density.

$\alpha$ = Ratio of absorption to scattering cross sections at the energy $kT_0$.

The integral (1) was evaluated by the method of partial fractions for a peak energy $E_n$ = 0.0302 ev and gave an age contribution of $\Delta\tau^F$ = 64.8 $cm^2$. This gives a total Fermi age in graphite of 336.6 $cm^2$.

Since the reactors considered contain appreciable void and metal, the Fermi age in graphite is corrected by the formula

$$\tau^F = \tau^F/(1 - VF_m)(1 - VF_v)^2 \quad , \tag{3}$$

where

$\tau^F$ = Fermi age in graphite, 336.6 $cm^2$

$VF_m$ = Volume fraction of metal in core

$VF_v$ = Volume fraction of void in core.

The reactor age for the epithermal group was obtained by correcting the value $\Delta\tau^F = 64.8$ $cm^2$ by means of Equation (3). The reactor age for the high-energy group was then found by equating the three-group criticality expression to the Fermi-age critical equation and solving for $\tau_R$ for the fast group.

The thermal-group cross sections were obtained by averaging energy-dependent cross sections over the neutron energy spectrum calculated from the infinite medium, heavy gas model, using the definition of absorption parameter $\Delta = 2m\alpha$ given in Reference (12).

(2) A twenty-six group diffusion theory calculation, using twenty-five fast groups down to 0.4 ev and one thermal group. The neutron slowing-down (group-removal) cross sections for carbon were calculated from the relation

$$\sigma_{\text{el mod}}^{(j \rightarrow j+1)} = \frac{\xi\sigma_{tot}}{\Delta u} \quad ,$$

where

$\xi$ = Average logarithmic energy decrement per collision

u = Lethargy width of group j.

A neutron was assumed to enter the thermal group upon crossing the 0.4-ev lower limit on the energy of the 25th group. For a graphite density of 1.71 g/cc, the Fermi age ($\tau^F$) down to indium resonance energy, which one deduces from the multigroup cross sections, is 259.3 $cm^2$, compared to the measured value of ~272 $cm^2$ which went into the three-group calculation. Below indium resonance energy, the 26-group cross sections yield a value for $\Delta\tau^F$ of 38.6 $cm^2$, compared to the increment of 64.8 $cm^2$ utilized in the three-group calculation. Hence, the $\tau^F$ to "thermal" in the 26-group calculation was 11 per cent less than that of the three-group calculation, which difference affected both criticality and spectral considerations.

The thermal group in the 26-group calculation was the same as in the three-group set.

(3) A twenty-group calculation, in both the diffusion and $S_n$ approximation, employing a single fast group down to 2 ev and the gas model for energy exchange between graphite and neutrons of energy within the 19 thermal and near thermal groups. The group energy breakdown used is listed in Table V.

Table V

ENERGY BREAKDOWN OF TWENTY-GROUP, GAS MODEL CROSS SECTIONS

| Group | Lower Limit of Group Energy, ev | Group | Lower Limit of Group Energy, ev |
|---|---|---|---|
| 1 | 2.00 | 11 | 0.2 |
| 2 | 1.5 | 12 | 0.15 |
| 3 | 1.0 | 13 | 0.1 |
| 4 | 0.8 | 14 | 0.07 |
| 5 | 0.6 | 15 | 0.05 |
| 6 | 0.5 | 16 | 0.04 |
| 7 | 0.4 | 17 | 0.03 |
| 8 | 0.35 | 18 | 0.02 |
| 9 | 0.3 | 19 | 0.01 |
| 10 | 0.25 | 20 | $3.00 \times 10^{-6}$ |

Slowing down from the fast group, in this 20-group set, was identical to that used out of the fast group in the three-group set discussed earlier, except for a correction due to change in energy of the lower group limit from 1.44 to 2.0 ev. There was no scattering upward, into group 1, from lower energy groups.

Due to limitations imposed by available computing programs, inelastic scattering was permitted from any group only into its five closest neighbors on either side of it, energywise. Coefficients calculated for groups beyond this range, which were generally quite small, were lumped into the coefficients for scattering into the fifth group.

A close approximation to the actual flux shape was used for averaging cross sections within a group. A new program, devised by V. Z. Jankus, et al.,[13] permits the neutron density within each group to vary as a Maxwellian with arbitrary coefficient in the exponential, or as a power of neutron velocity with arbitrary exponent. By precalculating the approximate spectrum, using the heavy gas model,[12] a good fit within each group was possible.

The group scattering cross sections for carbon were compared with those obtained using the assumption of constant neutron density with the following results for the ten higher energy groups:

1) $\sigma_{j \to j}$ (scattering by a group into itself) differed by 6% for groups 2 and 3, agreed within 1% for lower energies.

2) $\sigma_{j \to j+1,\ j+2,\ j+3,\ \text{etc.}}$ (scattering into lower energy groups) varied 10-20 per cent for groups 2 and 3, agreed within a few per cent for lower energies.

3) $\sigma_{j \to j-1,\ j-2,\ \text{etc.}}$ (scattering upward in energy) varied about 20% for group 3, and maintained a many per cent variation for several lower energy groups.

No reactor calculations were made using the graphite cross-section matrix obtained with the assumption of constant neutron density within each group. Small differences in the theoretical prediction of temperature coefficient or prompt neutron lifetime with the two graphite scattering matrices would have been subject to major uncertainties due to convergence difficulties explained below in the section of neutron lifetime.

## C. Criticality Calculations

The difficulties experienced in getting two and three-group calculations to agree with nearly homogeneous, reasonably well thermalized, graphite-moderated critical experiments have been reviewed by Iskenderian.[5] In those calculations, the heavy gas model was used to assign a neutron temperature to the thermal group, and the increment in slowing-down length between the indium resonance (1.4 ev) and thermal energy was taken as the adjustable parameter. Iskenderian found that neither the prescription of Cohen[12] nor that of Hurwitz, Nelkin and Habetler[14] gave agreement with some critical experiments performed at Los Alamos,[5] and that they even disagreed with each other. It was then found that the semi-empirical age ($\tau$) derived from the Los Alamos criticals fit the TREAT critical, after allowance for boron in the core graphite was made.[6]

As noted by Iskenderian[5] the study of homogenous, graphite-moderated assemblies becomes further aggravated when some bare critical experiments performed by UCRL, Livermore, are included in the analysis. If the methods of analyses utilized by Iskenderian are sufficiently accurate, the Los Alamos and Livermore sets of experiments seem incompatible with each other.

A partial explanation of the difficulties experienced by Iskenderian may lie in the inadequacies of the few-group method. Radial reflector savings calculations for a TREAT-like reactor were made using two-group

and twenty-six group calculations, where each calculation used the same thermal group, but the fast group was divided into 25 for the multigroup case. The 26-group case gave a reflector savings of 30.2 cm, which was 1.5 cm less than that of the two-group calculation. This difference in reflector savings has the same effect on reactivity as a 5% change in $\tau$, and may be part of the reason that the two- (and three) group calculations need a relatively large $\tau$ to fit experiment.

When criticality was determined using the 20-group, gas model calculation with a fast group $\tau$ compatible with experimental measurement down to indium resonance energy,(11) the theory led to considerably more reactivity than experiment (giving a calculated $k_{eff}$ = 1.028 for a spherical approximation of the critical configuration). This could be due in part to the inadequacy of the single fast group, as mentioned previously. The three-group calculation of the same configuration, using a $\tau$ which fit the Los Alamos criticals, yielded a value for $k_{eff}$ of 1.005. It is of interest to note that when the 20-group, gas model cross sections were collapsed to a new three-group set, using the core spectrum of the specific TREAT configuration to weight the various groups, this new set, which allowed for scattering from the thermal to the epithermal group, and whose effective $\Delta\tau$ from indium resonance to thermal was that prescribed by the gas model, gave a value for $k_{eff}$ of 1.025, nearly identical to the prediction of its parent 20-group set.

A few additional comparisons between experiment and the results of simple criticality calculations are of interest in evaluating the reliability of theoretical techniques. The effect of core radius on excess reactivity has been measured for the simple cylindrical reactor; the experimental results, as shown in Fig. 7, are in excellent agreement with the predictions of the three-group calculation normalized to criticality by the method of Iskenderian.

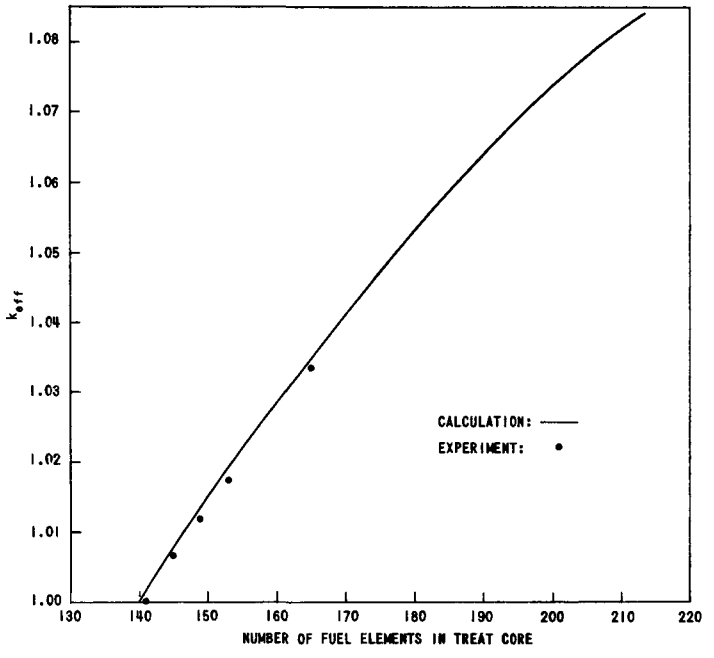


FIG. 7
MULTIPLICATION FACTOR, $k_{eff}$, VS. CORE SIZE

Radial and axial fission distributions measured with $U^{235}$ fission counters also compared reasonably well with theory. In Figs. 8 and 9, the results of 20-group gas model calculations in the radial and axial directions can be seen to lie close to the experimental points over the full range. Few-group calculations also

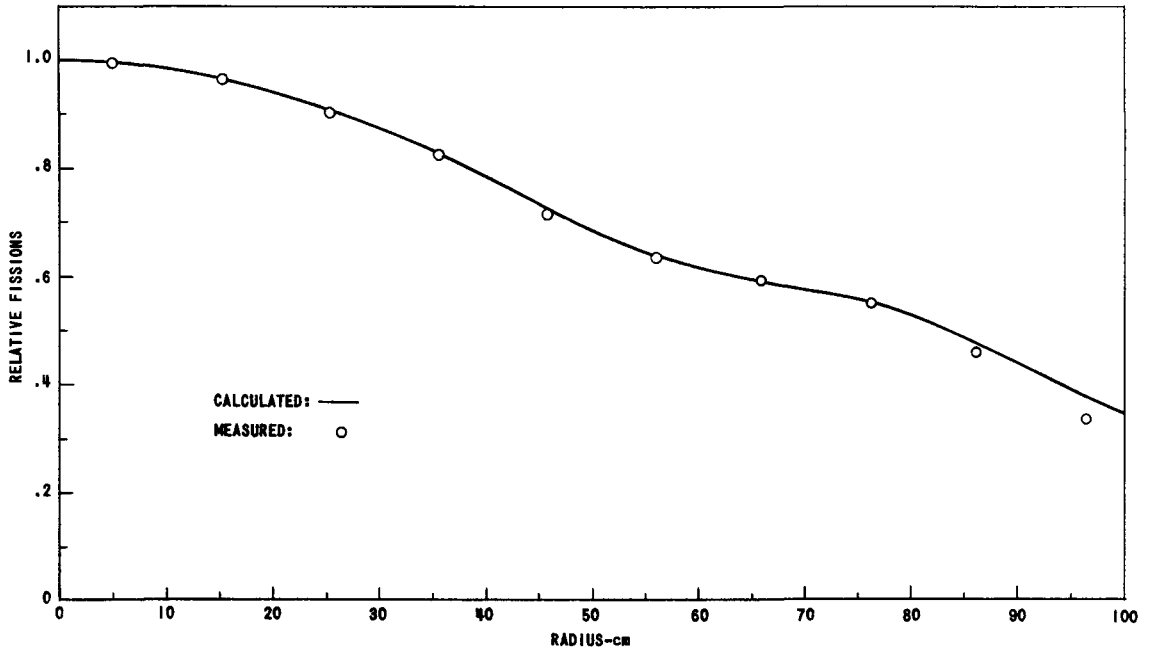


FIG. 8
RADIAL $U^{235}$ FISSION RATE IN TREAT

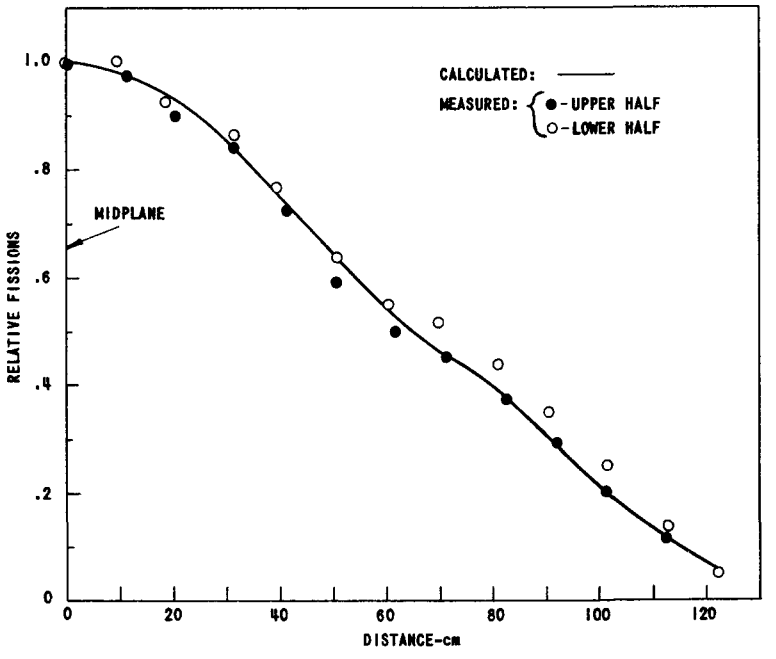


FIG. 9
AXIAL $U^{235}$ FISSICN RATE IN TREAT

gave fairly good agreement. The consistently higher axial data in the lower half of the reactor relative to the upper half is thought to be a real physical effect, caused by the presence of control rods in the upper reflector. Rough theoretical models of this effect produced similar differences.

## D. Neutron Energy Spectrum

Detailed measurements of the neutron energy spectrum in TREAT have not been made. What do exist are the relative fission rates of $Pu^{239}$ and $U^{235}$ and the cadmium ratio measurements with $Pu^{239}$, $U^{235}$ and copper. The fission ratio measurements, which were made as a function of position and at a few different moderator temperatures, provide a test of the shape of the thermal and near-thermal flux curves, due to the large plutonium resonance at 0.3 volt, while the cadmium ratio measurements are primarily a test of the ratio of fast to thermal flux.

Both the three-group and 20-group calculations employed a single fast group, with an effective age ($\tau$) adjusted to equate $1 + \tau B^2$ and $e^{\tau_F B^2}$, where $\tau_F$ is the so-called Fermi age.[5] For the three-group case, the scattering out of the second group is adjusted to fit criticality, whereas in the 20-group calculation the prediction of the gas model is accepted. Both these calculations gave relatively poor agreement with measurements of cadmium ratio, as is summarized in Table VI.

Table VI

CADMIUM RATIOS

| Sample | Measured Cadmium Ratio | 3-group Calculation | 20-group Calculation | 26-group Calculation |
|---|---|---|---|---|
| Cu | 9.2 ± 0.5 | 7.4 | 8.4 | 9.2 |
| $U^{235}$ | 18.3 ± 1 | 11.7 | 13.8 | 15.7 |
| $Pu^{239}$ | 19.5 ± 1 | 13.8 | 15.6 | 19.9 |

It was believed that a calculation with age ($\tau$) adjusted to fit criticality could easily lead to a poor prediction of the ratio of fast to slow flux. Hence, following a suggestion by H. H. Hummel, the 26-group cross-section set, using 25 fast groups to simulate closely the continuous slowing-down picture of graphite, was employed to calculate the TREAT spectrum, resulting in a considerable improvement in agreement with cadmium ratio measurements.

It is noted that the cadmium ratio calculation for copper is based on the resonance integral measurement for copper reported by H. Rose, et al.(15) Use of the older values reported in ANL-5800(16) would result in a cadmium ratio about 15% smaller.

The calculation of the ratio of fission in $Pu^{239}$ to that in $U^{235}$ was done in two distinct ways. The simpler calculation used the 26-group set which has 25 fast groups coupled to a thermal group covering the energy range below 0.4 ev, where the thermal spectrum was taken from the heavy gas approximation of Cohen.(12) By this method a fission ratio for $Pu^{239}$ relative to $U^{235}$ at the core center of 1.65 was predicted, which is in very good agreement with the measured value of 1.62.(9)

The more involved calculation employed the gas model with one fast group and 19 thermal groups in the energy range below 2 ev. Calculations were made both for the finite, reflected reactor and an infinite medium representative of the core.

When the many-group gas model calculation for an infinite medium, performed by an SNG program, was compared with the prediction of the heavy gas model solution,(12) a small but definite discrepancy was noted. This is illustrated in Fig. 10, where the dashed curve (No. 1) represents the standard prediction of the neutron spectrum given by the infinite medium, heavy gas model, while the points designated by an encircled "x" represent the calculated points from the many thermal group, infinite medium gas model solution.

V. Z. Jankus suggested that this discrepancy, which manifests itself primarily in the amount of a $1/E$ tail relative to the near-Maxwellian peak, resulted from the definition of the absorption parameter $\Delta$, which is defined by Cohen as $2\,m\alpha$, where m is the moderator mass in units of the neutron mass, $\alpha$ is the ratio of absorption to scattering cross sections at the energy $kT_0$, and $T_0$ is the moderator temperature. Jankus's reasoning is as follows:

We know that the number of neutrons slowed down per second and per $cm^3$, q (past a certain lethargy u, far from the first collision), is given by

$$q = \xi \Sigma_s \phi(u) \quad , \tag{4}$$

where $\Sigma_s$ is the scattering cross section, $\xi$ is the average logarithmic decrement, and $\phi(u)$ is the neutron flux per unit lethargy interval, which is essentially constant at high energies where absorption is negligible.

If we assume the absorption cross section is inversely proportional to the neutron velocity,

$$\Sigma_a = \alpha\Sigma_s \sqrt{kT_0/E} = \alpha\Sigma_s (1/x) \quad ,$$

where x is the velocity variable normalized to unity at the velocity corresponding to the energy $kT_0$, we may write that the neutrons absorbed per second per $cm^3$ is given by

$$A = \int \Sigma_a \phi(u)du = \alpha\Sigma_s \int \frac{1}{x}\phi(x)dx \quad . \tag{5}$$

Equating (4) and (5), we have

$$\xi\Sigma_s\phi(u) = \alpha\Sigma_s \int \frac{1}{x}\phi(x)dx \quad , \tag{6}$$

where the equality holds at a high neutron energy. Now, since

$$\phi(u) = \phi(x)\left|\frac{dx}{du}\right| = \phi(x)\cdot\frac{x}{2} \quad ,$$

Equation (6) can be rewritten as

$$\lim_{x\to\infty}\left\{x\phi(x)\right\} = 2\frac{\alpha}{\xi}\int_0^\infty \phi(x)\frac{1}{x}dx \quad ,$$

or in terms of the neutron density as

$$\lim_{x\to\infty}\left\{x^2 N(x)\right\} = \frac{1}{2}\frac{4\alpha}{\xi}\int_0^\infty N(x)\,dx \quad . \tag{7}$$

Equation (7) is valid wherever the absorption cross section is $1/v$, irrespective of the details of the scattering cross section, provided only that it approaches scattering by a free atom at sufficiently high energies. If one then compares Equation (7) with Equation (18) of Reference 12, he finds that $\Delta = 4\alpha/\xi$, which differs from the heavy gas approximation used by Cohen ($\Delta = 2\ m\alpha$) in that $\xi = \frac{2}{m + 2/3}$, very closely.

When the infinite medium, heavy gas model calculation was redone with the Jankus definition of $\Delta$, it gave better, although not perfect, agreement with the SNG, many-group gas model calculation. This can be seen in Fig. 10 by comparing the SNG points with curve 2.

The spectrum at the center of the actual TREAT reactor, with finite core and fully reflected, was calculated with the many-thermal group, gas model by means of the Fire code.[17] The results are seen in the full curve, #3, of Fig. 10. A considerably higher tail results here due to leakage from the finite reactor system.

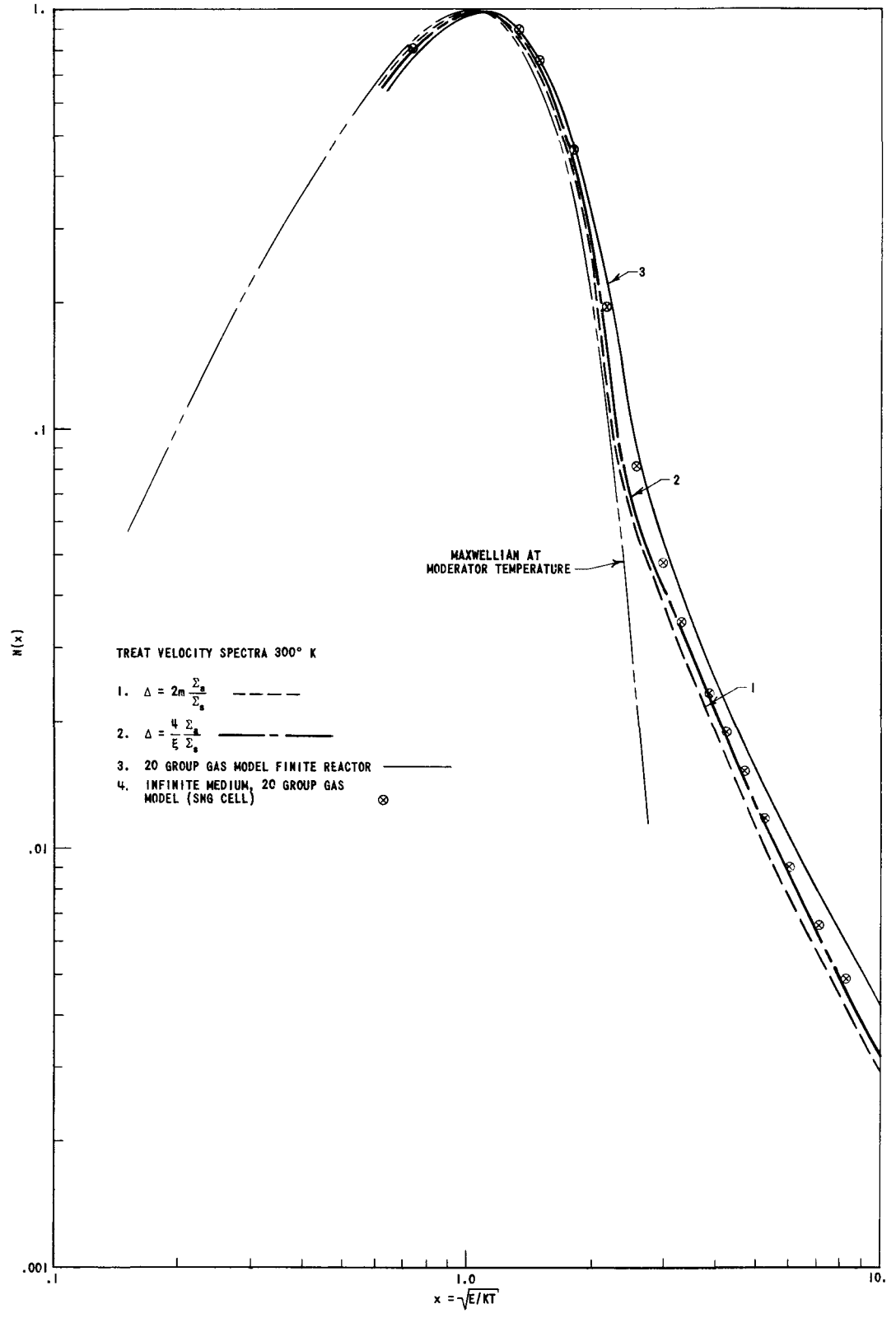


FIG. 10
NEUTRON ENERGY SPECTRUM AT CORE CENTER

The gas model calculation, for the finite reactor, predicted a somewhat higher ratio of fission in $Pu^{239}$ to that in $U^{235}$ than was measured. At the core center a ratio of 1.74 was calculated, compared to the experimental value of 1.62. The calculation was performed for a range of core moderator temperatures, and is compared with experiment over a limited temperature range in Fig. 11. Reasonably good agreement on shape was obtained, a generally increasing ratio with core moderator temperature resulting. This is at variance with the results of some calculations by Meneghetti and Phillips[18] on a hypothetical TREAT-like reactor with a slightly lighter uranium loading (ratio of carbon atoms to $U^{235}$ atoms = 12,500). As is shown by the dashed line in Fig. 11, they obtained a reversal of slope at low temperatures. The reason for the discrepancy is not clear, since the work in Reference 18 is reported to be based on the heavy gas model.

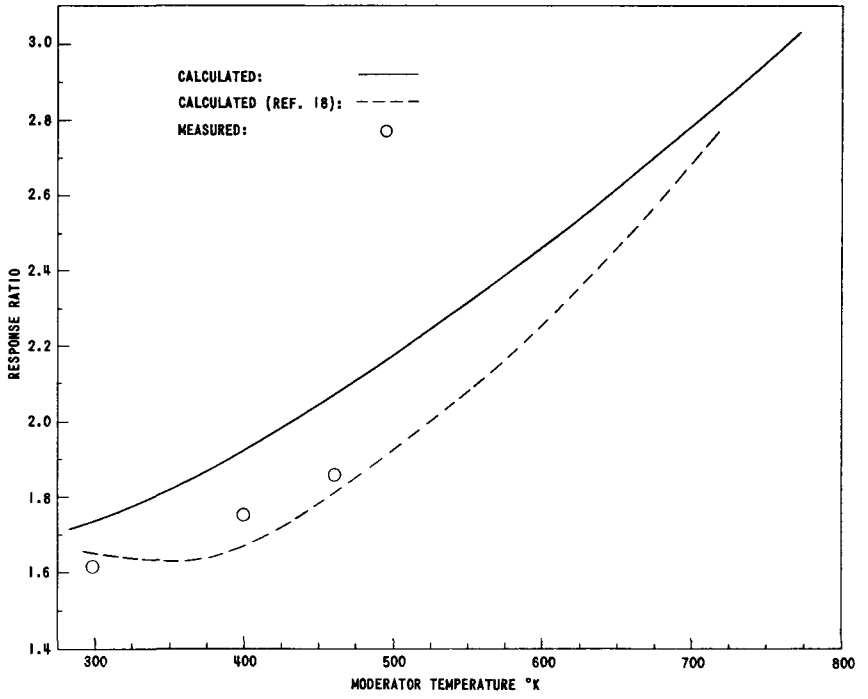


FIG. 11
$Pu^{239}/U^{235}$ FISSION RATIO VS.
MODERATOR TEMPERATURE AT CORE CENTER

Actually, there exists additional experimental evidence, confirming the TREAT experimental trend, in the work of Stinson, et al.,[19] on this fission ratio as a function of moderator temperature.

Axial distributions of the ratio of $Pu^{239}$ to $U^{235}$ fissions were measured at a 300K moderator temperature, and also with a temperature distribution through the core and reflector. Gas-model calculations were made in spherical geometry, employing an "axial-type" reflector, and the spectral variations with position transformed into predictions of the fission

ratio. The results of theory are compared with experiment in Fig. 12 for the uniform, room temperature case, and in Fig. 13 for the elevated temperature condition. In the latter case, the temperature variation in the core was approximated by two steps. The agreement is fair as regards shape, the shift at the core center holding the calculated ratio above experiment throughout.

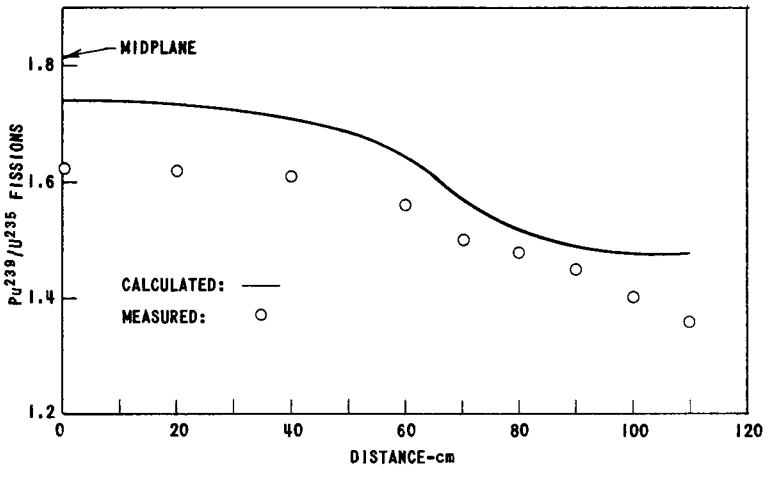


FIG. 12
AXIAL VARIATION OF $Pu^{239}/U^{235}$ FISSION RATIO
(MODERATOR TEMPERATURE 300°K)

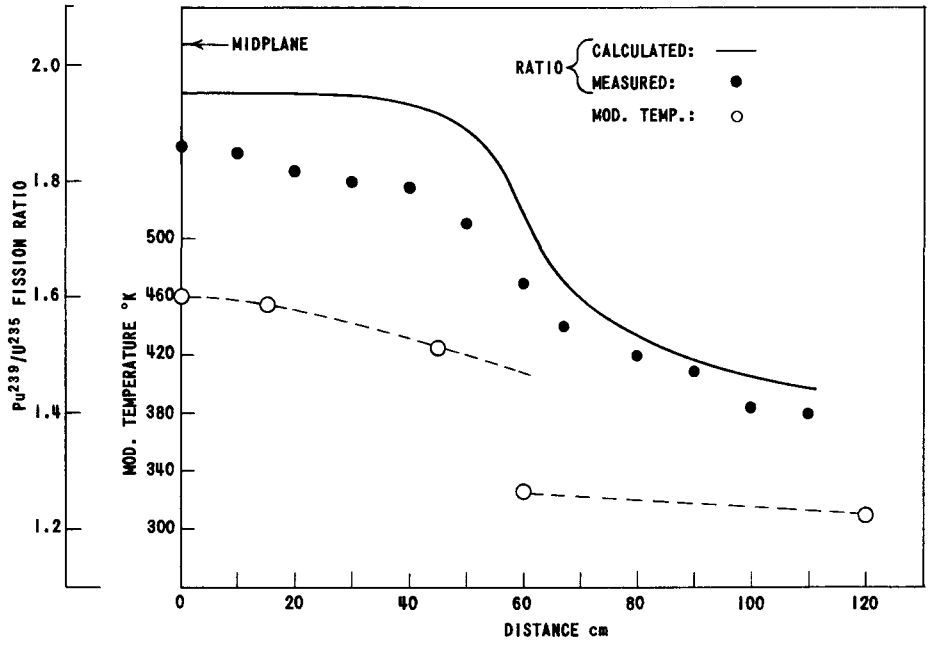


FIG. 13
AXIAL VARIATION OF $Pu^{239}/U^{235}$ FISSION RATIO
FOR NON-UNIFORM MODERATOR TEMPERATURE

## E. Prompt Neutron Lifetime

The prompt-neutron lifetime was calculated using both the three-group model and the 20-group gas moderator model. In each case the change in reactivity of the reactor with the uniform addition of a small amount of 1/v-absorber was calculated, and the prompt-neutron lifetime determined from the relation

$$\ell = \frac{\delta k}{v \, \delta \Sigma_{capture}} \quad .$$

For the three-group calculation, a spherical, homogenous core, surrounded by a 95-cm thick reflector composed of normal aluminum-clad dummy elements, was chosen as the reactor model. A neutron lifetime of $8.7 \times 10^{-4}$ sec resulted, in good agreement with the measured results of $(9.0 \pm 0.3) \times 10^{-4}$ sec.[9]

Using a reactor model similar except that the reflector had a volume-averaged composition, a prompt-neutron lifetime of $7.5 \times 10^{-4}$ sec was originally calculated[8] using the Fire code and the 20-group gas model cross sections. However, subsequent use of the Fire code proved that the convergence on the eigenvalue had been poor in this particular reactivity calculation.

The first calculations were performed with the convergence criterion $\epsilon$ (where $\epsilon$ is the difference in $k_{eff}$, the eigenvalue, for two successive iterations) set at $1 \times 10^{-4}$. Flux guesses were made based on a previously solved problem of similar geometry. When some unexplainable differences occurred on rerunning certain problems, the adequacy of convergence became suspect, and one problem was run to a convergence criterion of $1 \times 10^{-6}$. The variation of eigenvalue is plotted against $\epsilon$ in Fig. 14. It can be seen that between an $\epsilon$ of $1 \times 10^{-4}$ and one of $1 \times 10^{-5}$, $k_{eff}$ changed from 1.0275 to 1.0255, with a smaller, monotonic shift thereafter.

The prompt-neutron lifetime calculation for 300K moderator was therefore rerun with a tighter convergence criterion ($\epsilon = 10^{-5}$) and considerably greater apparent success was obtained; a value of $\ell = 9 \times 10^{-4}$ sec gave excellent agreement with experiment. Further work has shed some doubt on this agreement, however.

It was of interest to know how the prompt neutron lifetime would vary with core moderator temperature, since this could affect the detailed shape of the power curve in a burst. Measurements at two slightly different temperatures by the transfer function technique were inconclusive, except that the lifetime seemed not to vary within accuracy limits of the measurement.[9] Calculations with the 20-group cross sections were

performed using the 1/v-absorber method, and somewhat anomalous results were obtained. While there seemed to be some trend toward decreasing the lifetime with increase in core moderator temperature (~10% in 300°K), there was a considerable scatter about a smooth curve. It was found upon further testing that the $k_{eff}$ eigenvalue was sensitive to the choice of initial flux guess, as well as the convergence criteria, and that a difference of ~0.001 $\delta k/k$ could result in problems run with an $\epsilon$ of $1 \times 10^{-5}$. This leads to an uncertainty of 5-10% in the lifetime calculations, as run herein, and produced both the observed scatter and a doubt in the validity of the agreement with experiment at room temperature.

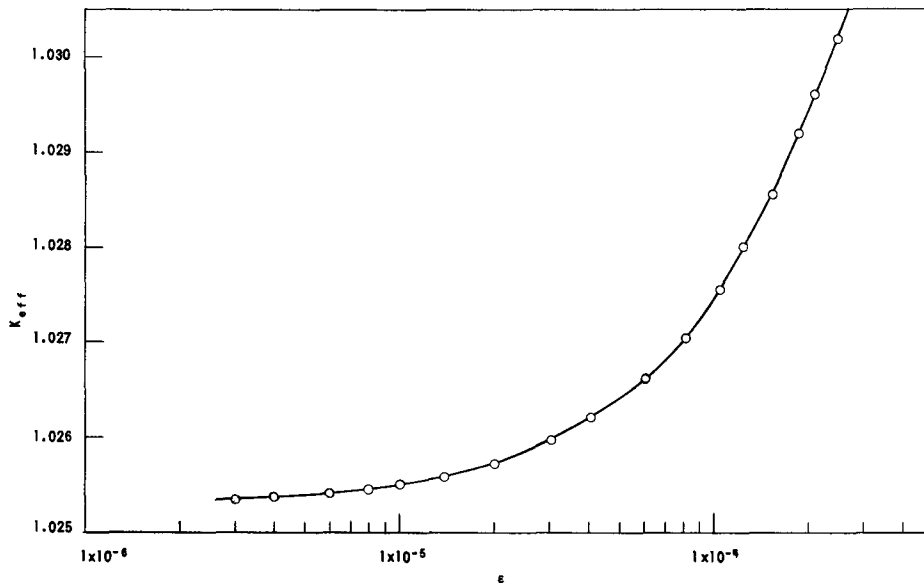


FIG. 14
$K_{eff}$ VS ε, THE CONVERGENCE CRITERION FOR THE FIRE CODE

## F. Temperature Coefficients

Measurements have been made of the effect on reactivity for a nearly isothermal temperature change, and for a temperature change which had nearly the same shape as the power distribution.(9) The isothermal change, made over a relatively small temperature shift and therefore having a considerable uncertainty, resulted in a value of $-(1.8 \pm 0.2) \times 10^{-4}$ $\delta k/k$ per °C. The reactivity effect in the nonisothermal case, which was measured by heating with no coolant flow, resulted in a value of $-1.3 \times 10^{-4}$ $\delta k/k$ per °C change at the core center. On applying the measured maximum-to-average flux ratio for the core, one obtains a value of $-2.2 \times 10^{-4}$ $\delta k/k$ per average °C change in the core. These experimental values agreed closely with the preliminary values reported earlier.(7,8) It is of interest to note that the measurement under power, which covered the range roughly from 60°C to 170°C, yields an almost constant coefficient, within experimental error, except for the first 20°.(9)

The calculations of temperature coefficient employing the 20-group, gas model cross sections are in fairly good agreement with experiment, both qualitatively and quantitatively. The calculated effect of reflector heating is opposite in sign to that of the core, so that the coefficient for core heating alone is more negative. Furthermore, the calculated isothermal coefficient near room temperature is $-1.7 \times 10^{-4}\ \delta k/k$ per °C, in excellent agreement with experiment.

For uniform heating of the core over the same temperature range as experiment, with no reflector heating, however, a coefficient of $-2.5 \times 10^{-4}\ \delta k/k$ per average °C is obtained; when a correction for nonuniformity of heating is calculated, this value is increased about 10% to $-2.8 \times 10^{-4}\ \delta k/k$ per average °C. This latter value is about 25% higher than the experimental value reported in Reference (9) and which is deduced later on in this report in the burst studies.*

The calculated temperature coefficient for uniform core heating with no reflector heating is plotted over a wide temperature range in Fig. 15. It is noted that the curve departs somewhat from linearity, even over the limited range of experimental measurement.

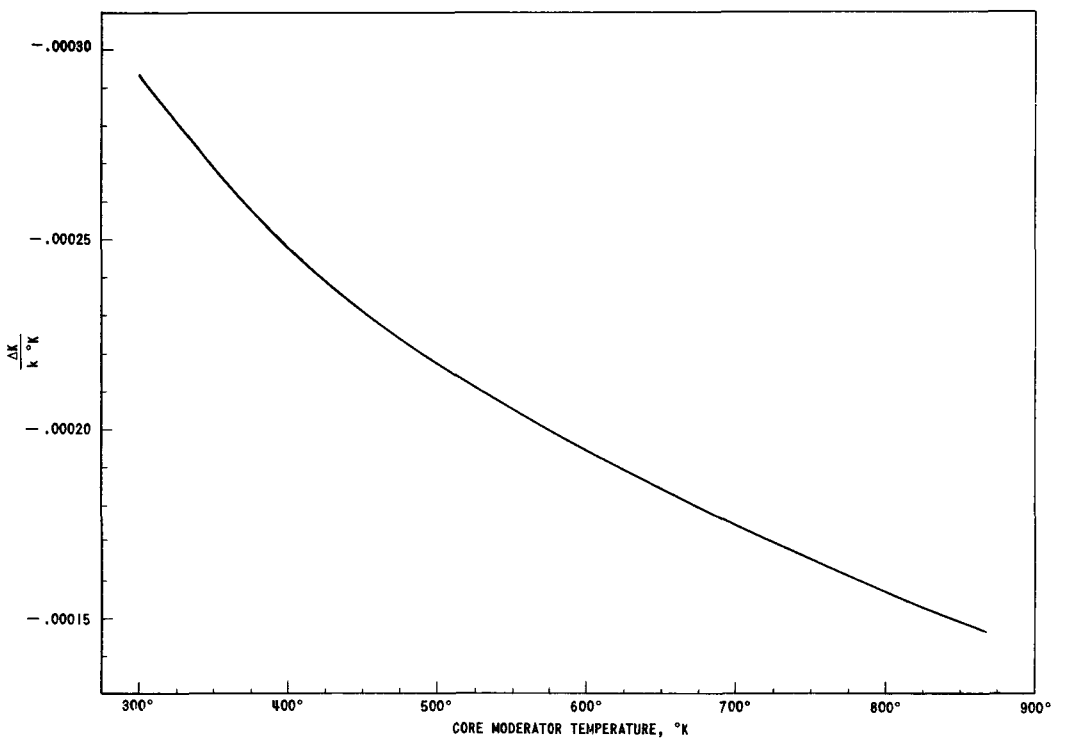


FIG. 15
20 GROUP GAS MODEL PREDICTION OF TEMPERATURE COEFFICIENT OF REACTIVITY VERSUS CORE MODERATOR TEMPERATURE
(UNIFORM CORE TEMPERATURE, REFLECTOR AT 300°K)

*It is noted that the preliminary value of $-3.2 \times 10^{-4}\ \delta k/k$ per average °C for nonuniform heating reported in Reference (8) was found to be in error due in part to the poor convergence characteristics of the Fire code as discussed earlier.

Temperature coefficient calculations were also made using the three-group method, by computing thermal group cross sections by the heavy gas approximation for several temperatures and adjusting the slowing down from epithermal to thermal group accordingly. For uniform core heating and maintaining the room temperature thermal group in the reflector, about the same average temperature coefficient was obtained for the range from 300 to 500°K. The coefficient showed about twice the departure from linearity obtained with the 20-group, gas model calculations, however.

Iskenderian[5] obtained the same coefficient of $2.5 \times 10^{-4}$ $\delta k/k$ per °C by perturbation methods for an equivalent bare reactor, using the Wescott data, for the slightly greater temperature range of 300-600°K. Since the reflector is observed and calculated herein to produce an appreciable reduction in the temperature coefficient, the apparently good agreement between calculations is subject to some uncertainty. Iskenderian did find an appreciable dependence of the temperature coefficient on moderator temperature, in agreement with the predictions of the 20-group gas model.

# II. ANALYSIS OF TREAT TRANSIENTS

## A. Introduction

In principle, the transient behavior of TREAT should be amenable to description by the standard one-energy group reactor kinetics equations and a single, prompt negative temperature coefficient of reactivity. The feedback mechanism is the change in $k_{eff}$ brought about by the hardening of the neutron energy spectrum due to a rise in moderator temperature, the principal effect being an increase in neutron leakage from the core as the neutron temperature rises.

The first step in analyzing the transient behavior of TREAT consisted of obtaining experimental feedback data. Values of reactor neutron density as a function of time were taken from the oscillograph traces of transient power. The neutron-density information was analyzed with the aid of an electronic computer, using the measured value of prompt-neutron lifetime and calculated effective delayed-neutron fractions, to obtain reactor $k_{ex}(t)$ and thus $k_{ex}$ as a function of integrated neutron density or temperature, during the transients. Because of scatter in these derived values of feedback, this step was used only for orientation.

Next, the experimental power traces were compared with theoretical calculations of reactor power, which were based on calculations of $k_{eff}$ as a function of core temperature for a TREAT-like system, the measured prompt-neutron lifetime, the calculated effective delayed-neutron fractions, and the measured specific heat of the fuel. The feedback was normalized to provide general agreement on peak power and this normalized feedback was then used in attempts to reproduce shapes of the power curves, integrated transient power values, and maximum reactor temperatures.

Satisfactory agreement was obtained between experiment and theory. Hence, theoretical calculations were extended to higher reactor temperatures than those encountered in the test transients, and estimates were made of reactor kinetics performance to be expected during more severe reactor transients.

## B. Experimental Data Reduction

### 1. Use of Data

Information on transients used in the study of the reactor transient kinetics consisted of the following data:

1) Oscillograph traces of transient output from four boron chambers in the reactor shielding - two chamber outputs

were amplified by linear amplifiers and were designated as Safety 1 and Safety 2; the other two outputs were amplified by log amplifiers and were designated as Log 1 and Log 2.

2) Oscillograph traces of transient output of three thermocouples in the reactor core, designated as TC-523, TC-531 and TC-551.

3) Total number of counts recorded in two $U^{235}$ fission chambers located in the reactor shielding.

4) Control rod positions.

Reactor power, as a function of time, was read from the oscillograph traces of the boron chamber outputs during each transient. The chamber calibrations are discussed elsewhere.[9] Prior to each excursion, the recording circuit for each chamber was calibrated by noting the oscillograph trace deflections produced by signals of known amplitude. Because of the necessity of referring records of transients to base line and calibration traces, data from the oscillograph records possess an inherent uncertainty of the order of the width of an oscillograph trace (or about 2-4% of the maximum deflection noted in typical cases). For linear instruments, like Safety 1 and Safety 2, this uncertainty is then approximately 2-4% of the maximum value recorded for a transient. However, such uncertainties in the log power instrument deflections would produce much larger ones in power values and, for typical cases, would correspond to an uncertainty of about 10%. Because of the relatively large uncertainties associated with the log power records, the log power recording circuits were calibrated only once each decade.

Thus, the two types of power instruments are complementary. Since there is a wide power range available on the log power records, they are useful for determining the values of initial periods, the general characteristics of transient power curves, and power levels near the end of the transients. The $k_{ex}$ calculations made from log power data would be expected to be of use principally to obtain initial $k_{ex}$, $k_{ex}$ as a function of time for the early and final portions of the excursions, and the general shapes of the $k_{ex}(t)$ curves. The linear (Safety) power records would yield the best values of maximum reactor power, and the best quantitative data on power near the maximum, i.e., within about one decade from the peak power. Calculations of $k_{ex}$ from the linear power traces would be the most reliable for $k_{ex}$ near the values at maximum transient power.

Direct comparison of the data from the four instruments on one graph for each excursion afforded a consistency check of calibration, zero shifts of recording circuits, and oscillograph record reading.

One method of obtaining integrated reactor power for the transients consisted of integrating the linear instrument data. The readings of

the two instruments were averaged, and small corrections were added where necessary for the initial and final portions of the transients using the log power records. This was the technique used to obtain values of power integrated to various times in the transients.

Core temperature rises noted by the reactor thermocouples also were used to calculate integrated transient power.[9] One thermocouple (TC-551) was located at a point at which the neutron flux was about $1\frac{1}{2}\%$ below the maximum for the reactor; its maximum readings were used, with a small correction for the difference in flux, to obtain maximum reactor temperatures. The maximum temperature rises recorded by TC-531 and TC-523 were compared against those of TC-551, as a check to insure that the core temperature records were consistent with the reactor power profiles. Data from TC-551 were not available for transients 4 and 15, and values of maximum reactor temperature for those two transients were calculated from the output of TC-523, which was located in a flux about 18% lower than the maximum. Again, uncertainties of the order of a few per cent are inherent in the records. The core thermocouples displayed an effective time constant of the order of seconds;[9] hence they were used only to obtain values of the integrated reactor power for complete transients.

A third way of measuring TREAT energy release was afforded by the two fission counters, whose outputs were recorded on scalers. The counters were positioned to give high sensitivity, without undue saturation, and total counts were high enough that typical standard deviations on the counter readings were of the order of 1% or less. However, the counters, which were located at opposite corners of the reactor shielding, appeared to be affected by flux tilting produced by control rods: insertion of the rods nearest counter 1 tended to decrease its counting rate, while raising that of counter 2. In typical cases, this effect was estimated to change the counting rates of a given counter by a few per cent. Uncertainties in the fission counter values for integrated power due to counting statistics and flux tilting were minimized by averaging the integrated powers from the counters.

Reported values of integrated reactor power for the test transients were obtained by combining data from the integrating fission counters, maximum core temperature rise, and numerical integration of the linear (Safety) instrument records.

TREAT control rods were calibrated in increments by the "rod bump" method.[9] Control rod positions were reported for the pre-transient criticality check and immediately before the transient rod was to be fired from the core. From these data it should be possible to obtain values of initial transient $k_{ex}$ from the previously prepared rod calibrations, independently of the initial $k_{ex}$ calculated from the asymptotic periods determined from the log power records. However, the original calibration was later found to be in error by 5%, introducing an uncertainty into such a procedure.

## 2. Calculations of $k_{eff}$

Initial reactivity and subsequent changes in reactivity during the test transients were calculated from the reactor power instrument readings, using the Argonne IBM-704 kinetics code RE-171.[20]* This computer code** solves the one-energy group, space-independent coupled reactor kinetics equations

$$\frac{\dot{n}}{n} = \left[ k_{ex}(1 - \beta_{eff}) - \beta_{eff} \right] \frac{1}{\ell} + \frac{1}{n} \sum_i \lambda_i c_i \qquad (8)$$

and

$$\dot{c}_i = n(1 + k_{ex}) \frac{\beta_{i\ eff}}{\ell} - \lambda_i c_i \,, \qquad (9)$$

where $\beta_{i\ eff}$ is the effective delayed-neutron fraction for the $i^{th}$ delayed group, $c_i$ is the concentration of the $i^{th}$ group precursor, and $\lambda_i$ is the decay constant for the $i^{th}$ group.

Four calculations of $k_{ex}$ as a function of time were made where possible for each test transient; one calculation for each of two linear power instruments and two log power instruments. The initial $k_{ex}$ for each excursion was determined from the calculations based on the log power records. At this stage of analysis, the absolute normalization of the individual instruments was not important, since the kinetics calculations depended on relative, not absolute, power (see Equations 8 and 9).

Figures 16, 17, 18, and 19 illustrate the ranges of applicability and degrees of agreement between the instrument data and the derived $k_{ex}$ values for two typical transients. Reactor power traces from transients initiated with $k_{ex}$ = 0.595% and 1.16% are shown in Figs. 16 and 17, respectively.*** Figure 18 shows the $k_{ex}$ calculations of the 0.595% $k_{ex}$ burst, and Fig. 19 presents the computer results from the 1.16% transient.

---

*Hence, the initial $k_{ex}$ values used in this report are those from RE-171 calculations, rather than those obtained from the asymptotic periods as determined directly from the recorder traces and reported in ANL-6173.

**This code is the IBM-704 version of the AVIDAC Code RE-31.[21]

***The values obtained directly from the period measurements from the recorder were 0.60% and 1.15% respectively.[9] This degree of agreement was typical of that for all transients except transient No. 5, for which the period determination gave 0.82%[9] and the RE-171 calculations gave 0.87%.

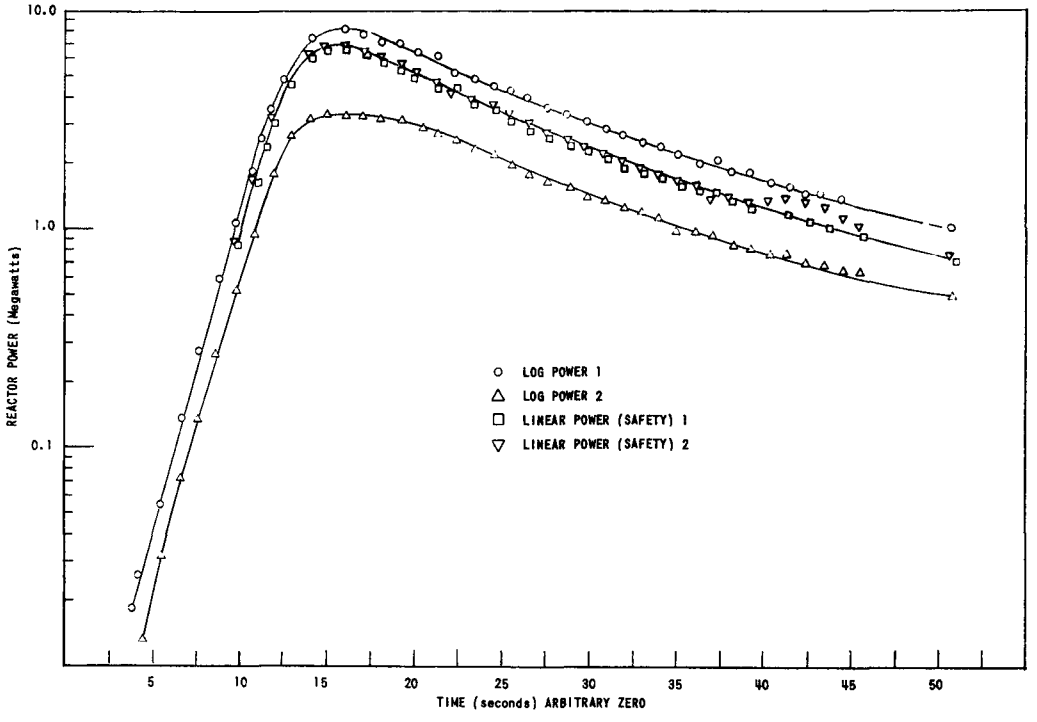


FIG. 16
POWER TRACES FOR 0.595% $k_{ex}$ TRANSIENT

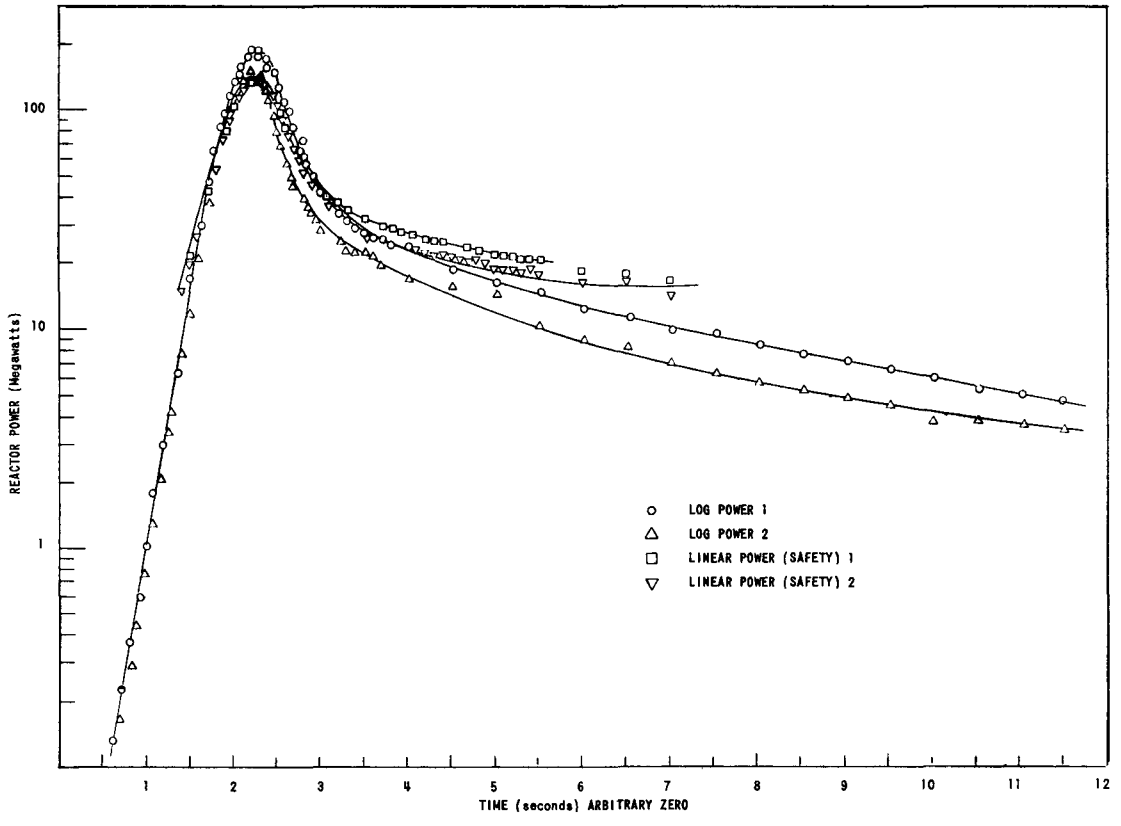


FIG. 17
POWER TRACES FOR 1.16% $k_{ex}$ TRANSIENT

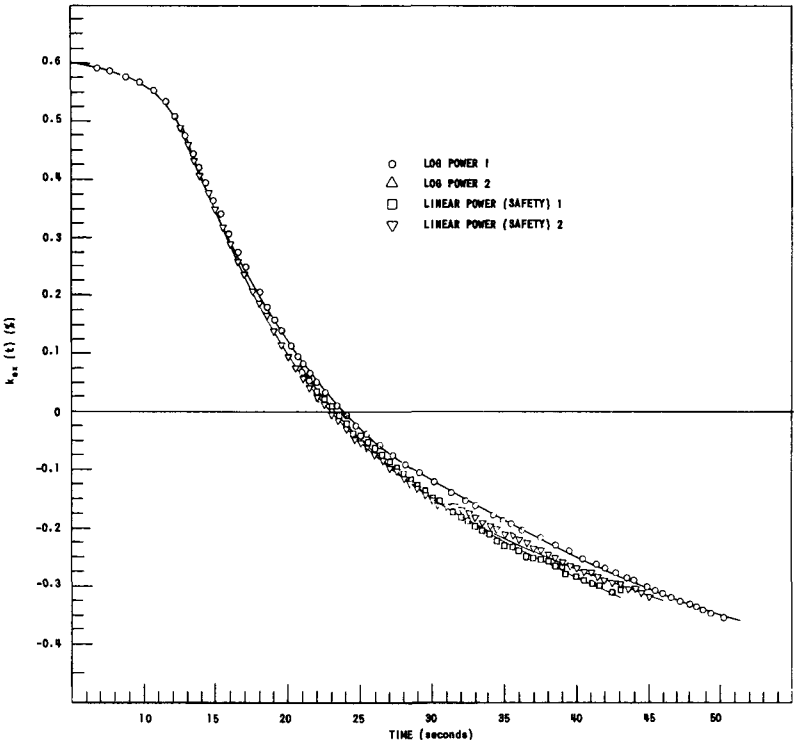


FIG. 18
$k_{ex}$ (t) CALCULATIONS FROM POWER TRACES OF FIGURE 16

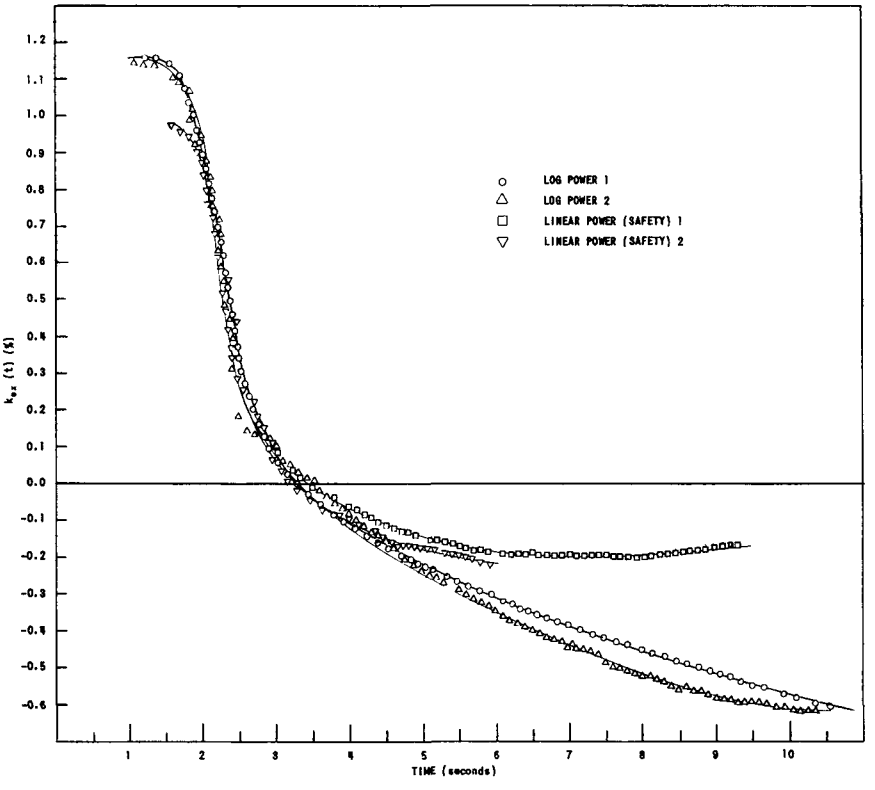


FIG. 19
$k_{ex}$ (t) CALCULATIONS FROM POWER TRACES OF FIGURE 17

The flattening of log power 2 noted in Fig. 16 is atypical and is attributed to an error in calibration. Because of it, no $k_{ex}(t)$ calculation was run for that power record. However, the trace was still useful for determinations of initial $k_{ex}$, initial and final portions of the power curve, and the general shape of the power curve. These figures demonstrate the wide range of data available from the log instruments, and the uncertainties in the data from the linear instruments at power levels below $\sim 1/10$ the peak power.

The value of lifetime used in the calculations was $8.8 \times 10^{-4}$ sec, the measured value reported previously.[7]* Effective delayed-neutron fractions were estimated for TREAT prior to criticality using the Keepin[22] delayed neutron data for $U^{235}$. Gwin's formula[23] was used to calculate the increased importance of the delayed neutrons, as compared with that of the prompt neutrons, which are produced at a higher energy and are thus more likely to leak from the core:

$$\frac{\beta_i}{\beta_{i\,eff}} = (1 - \beta) \exp \left[-(\tau_p - \tau_{di})\, B^2\right] + \beta \quad , \tag{10}$$

where $\beta_i$ is the delayed neutron fraction of the $i^{th}$ precursor group, and $\tau_p$ and $\tau_{di}$ are the Fermi ages of the prompt neutrons and delayed neutrons of the $i^{th}$ group, respectively. The $B^2$ used for these computations was that calculated for cold, clean, criticality: 0.000976 $cm^{-2}$.[5] Values of $\tau_p$ and $\tau_{di}$ were calculated for graphite by numerical integration of the formula for $\tau$, with first flight and last flight correction terms:[24]

$$\tau = \int_{E_1}^{E_2} \frac{dE}{3E\ \xi\ \Sigma_{tot}\ \Sigma_{tr}} + \frac{1}{3\,\Sigma^2_{tot}\,(E_1)} + \frac{1}{3\,\Sigma^2_{tot}\,(E_2)} \quad , \tag{11}$$

where $E_1$ is the neutron energy at birth, $E_2$ is the thermalization energy, and $\Sigma_{tot}$ and $\Sigma_{tr}$ are the total and transport cross sections, respectively, using the OCUSOL "eyewash" graphite cross sections.[16] Each $\tau_{di}$ for TREAT was then normalized to a reactor $\tau_p$ by multiplying the $\tau_{di}/\tau_p$ ratio for graphite by 540 $cm^2$, a semi-empirical value used in preliminary reactor calculations. The results of this computation are given in Table VII.

If one uses the measured cold clean critical value of $B^2$ = 0.000866 $cm^2$,[6] the calculated $\beta_{eff}$ is decreased 1.2%. Substitution of the semiempirical $\tau_p$ of 432 $cm^2$ calculated by Iskenderian[5] for cold clean criticality would decrease $\beta_{eff}$ by another 2.2%. Both corrections, however, would produce only a change in $\beta_{eff}$ of approximately the estimated ± 3% uncertainty in the Keepin $\beta$.[25]

---

*Recent re-evaluations of the lifetime measurements have resulted in the slight increase to $9.0 \times 10^{-4}$ sec.[9]

Table VII

DELAYED-NEUTRON PARAMETERS CALCULATED FOR TREAT

| Delayed Group Index Number i | Decay Constant $\lambda_i$, $sec^{-1}$ | Delayed-neutron Fraction $\beta_i$ | Mean Energy, kev | Age in Graphite, $cm^2$ | Age in TREAT, $cm^2$ | Effective Delayed-neutron Fraction, $\beta_{i,eff}$ |
|---|---|---|---|---|---|---|
| 1 | 0.0124 | 0.0021109 | 250 | 219.2 | 392.2 | 0.000244 |
| 2 | 0.0305 | 0.00140089 | 460 | 237.6 | 425.1 | 0.001567 |
| 3 | 0.1110 | 0.00125376 | 405 | 234.1 | 418.9 | 0.001411 |
| 4 | 0.3010 | 0.00252672 | 450 | 237.0 | 424.1 | 0.002828 |
| 5 | 1.1300 | 0.00073563 | 420 | 235.1 | 420.7 | 0.000826 |
| 6 | 3.0000 | 0.00026866 | 420 | 235.1 | 420.7 | 0.000302 |
| Prompt | | | | 301.8 | 540.0 | |
| $\beta = \Sigma_i \beta_i = 0.006397$ | | | | $\beta_{eff} = \Sigma_i \beta_{i\,eff} = 0.007178$ | | |

Both the Rossi-$\alpha$ and the zero-power transfer function measurements of TREAT prompt-neutron lifetime gave the same results within about 2%,(9) implying that the $\beta_{eff}$ used was, indeed, correct. However, the stated uncertainties in these measurements, ±5% and ±2%, respectively, would permit an uncertainty in $\beta_{eff}$ of about ±7%. A sensitive check of $\beta_{eff}$ can be made from the data for transients. It consists of comparing the values of initial $k_{ex}$ for super-prompt-critical transients as determined from RE-171 calculations on the asymptotic period regions with that determined from the control rod calibration.*

*This test is based upon the fact that the inhour equation has the asymptotic form, for super-prompt-critical periods of $k_{ex} \sim (\ell/T_p) + \beta_{eff}$ while, for large values of $T_p$, it has the asymptotic form $k_{ex} \sim \frac{1}{T_p} \Sigma \frac{\beta_{i\,eff}}{\lambda_i}$. Hence the control rod calibrations, which were done in increments by the "rod bump" method, were essentially proportional to the calculated value of $\beta_{eff}$. However, the super-prompt-critical period measurements gave values of $k_{ex}$ that asymptotically contained the calculated $\beta_{eff}$ as a term, not a factor.

Figure 20 gives the ratio of the two determinations of $k_{ex}$ for several test transients, assuming:

(1) $\ell$ = 8.8 x $10^{-4}$ sec and the $\beta_{i\ eff}$ for both the RE-171 calculations and the inhour to % $\delta k/k$ conversion of the rod calibration are those of Table VII.

(2) $\ell$ = 8.8 x $10^{-4}$ sec and the $\beta_{i\ eff}$ for both the RE-171 calculations and the inhour to % $\delta k/k$ conversion of the rod calibration are 17% larger than those of Table VII.

(3) $\ell$ = 8.4 x $10^{-4}$ sec and the $\beta_{i\ eff}$ for both the Re-171 calculations and the inhour to % $\delta k/k$ conversion of the rod calibration are those of Table VII.

For convenience in display, each ratio point is graphed against the initial $k_{ex}$ for that transient as determined from the rod calibration curve and the $\beta_{i\ eff}$ of Table VII.

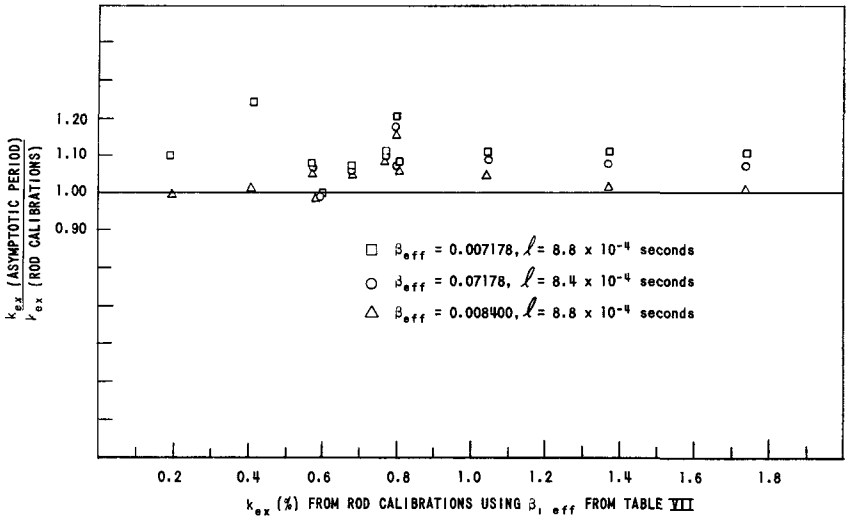


FIG. 20
COMPARISON OF INITIAL $k_{ex}$ FROM ASYMPTOTIC PERIOD WITH THAT FROM ROD CALIBRATIONS

The data of Fig. 20 suggested that the actual $\beta_{eff}$ in TREAT may be ~17% higher than that used (i.e., that of Table VII). However, the values of Table VII were used in the calculations because (1) the discrepancies observed in Fig. 20 actually are comparable to the estimated uncertainties in the rod calibration curve used;* (2) there was no supporting

*This calibration was repeated later, giving results that agreed much better with calculation.[9] However, although the repeated calibration could be expected to be more precise than that used for Fig. 5, it was done with a different core loading.

experimental evidence from the $\ell$ measurements; (3) the feedback relationship adopted gave a satisfactory fit to the entire range of transients; and (4) there are no good theoretical grounds for such a large increase in $\beta_{eff}$.

### 3. Conversion of TREAT Power to Neutron Density

Since the reactor power instruments are located away from the core in the reactor shielding, they do not give values of neutron density at locations in the core, but provide a measure of total reactor power. However, the kinetics calculations use neutron density and integrated neutron density, and the instrument readings must be converted into average specific power or average neutron density. For convenience, the core volume was expressed in number of fuel elements. The average neutron density, n, was determined by

$$n = P/K_p N_e \quad , \tag{12}$$

where

$P$ = reactor power in megawatts

$N_e$ = effective number of core elements

$K_p$ = (number of $U^{235}$ atoms/element) x $\sigma_f^{25}$ x ($2.2 \times 10^5$ cm/sec)

$$\text{x (Megawatts/fission)} = 3.232 \times 10^{10} \frac{\text{cm}^3}{\text{neutrons}} \frac{\text{Mw}}{\text{element}} \quad .$$

In a typical transient, the core size is somewhat larger than that necessary to initiate the burst. The surplus reactivity is compensated by control rods. Due to the flux depression in the regions of the rods, the core does not behave as if it were as large as indicated by the actual number of elements. In order to correct approximately the core to its effective size, the value of $N_e$ for a given transient was taken as the number required for the initial $k_{eff}$. The experimental data of Fig. 7 were utilized for this purpose.

## C. Theoretical Calculations of Feedback

### 1. Reactor Temperature as a Function of $\int n\, dt$

Calculations of TREAT temperatures as a function of integrated reactor power were based on the following assumptions:

1) Heat transfer from the uranium oxide fuel particles to the surrounding graphite matrix was essentially instantaneous.

2) No heat was lost from the uranium oxide-graphite system.

A time constant of 1.8 milliseconds has been calculated by MacFarlane[3] for transfer of heat energy from a 44-micron-diameter uranium oxide particle (maximum particle size for TREAT) through a 2-mil gas gap to graphite (estimate of the largest gap resulting from the fuel fabrication process). The shortest period for the test transients analyzed here was about 50 times this calculated time constant. Other heat transfer calculations had indicated the energy input to the TREAT core during a transient would be adiabatic. This prediction is borne out by experimental results,[9] as demonstrated in Fig. 21, which shows reactor core temperatures recorded at two points during the transients initiated with 0.595% and 0.87% $k_{ex}$.* The temperature traces show that the rates of heat loss from the instrumented positions, and the temperature redistribution between them, are much slower than the time scale of the power bursts - hence heat loss and temperature redistribution can be neglected for these transients. For simplicity, only two thermocouple positions, those of TC-551 and TC-523, are shown in Fig. 21. (The response time of the core thermocouples is slow enough to mask any urania-to-graphite time lag of the order of 1.8 millisecond.)

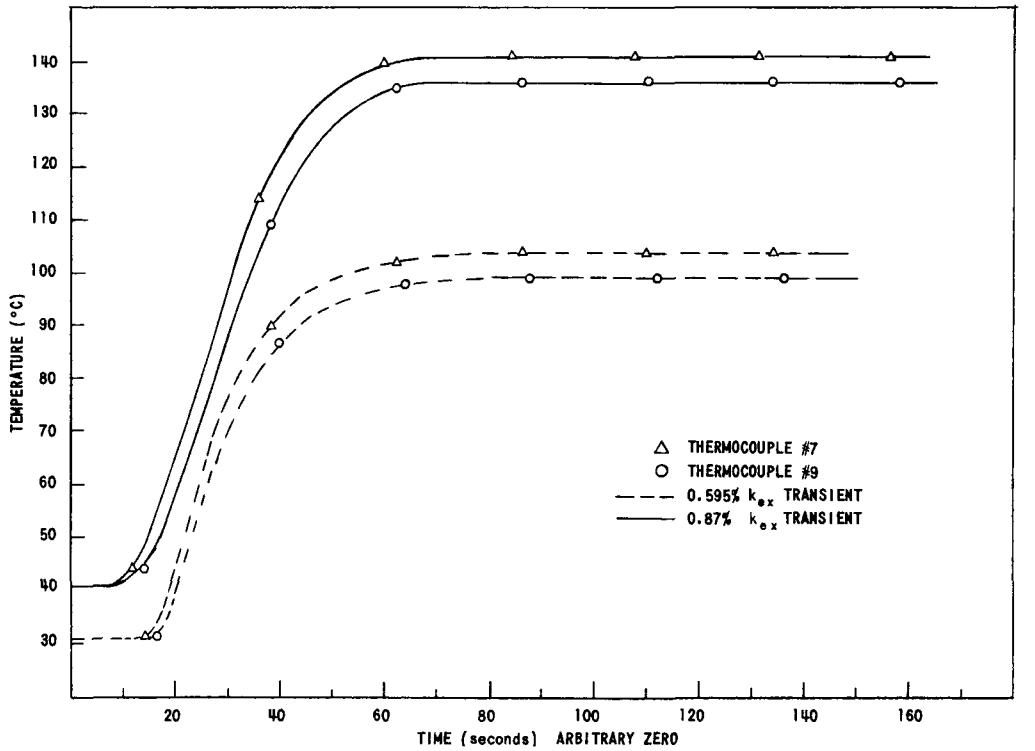


FIG. 21

TYPICAL CORE TEMPERATURE TRACES FROM THE 0.595% $k_{ex}$ AND 0.87% $k_{ex}$ TRANSIENTS

*The initial $k_{ex}$ values obtained from the period data taken directly from the recorder were 0.60% and 0.82%, respectively.[9]

Figure 22 gives the enthalpy of TREAT fuel with respect to 0°C, as determined by a least-squares fit to measurements by Battelle Memorial Institute.[26] For a 1/v fission cross section, the time-integrated neutron density in an increment of core material is proportional to the change in enthalpy producing the rise in temperature of the material.

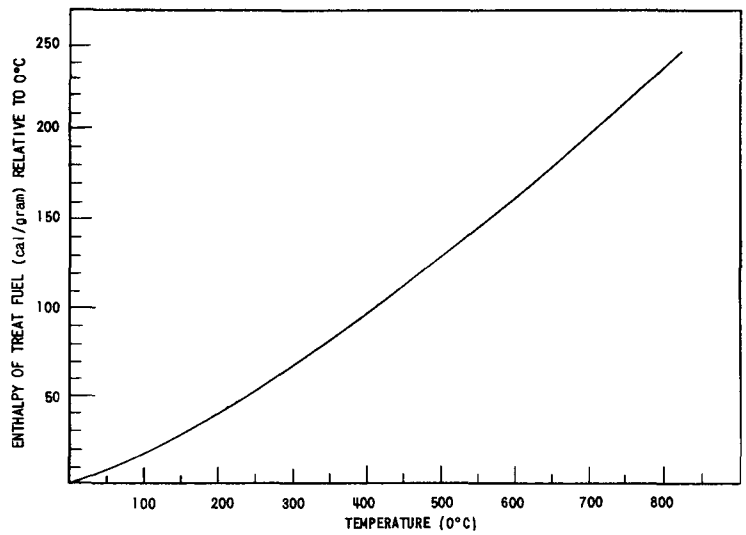


FIG. 22
TREAT FUEL ENTHALPY

Figure 23 shows the relationship between $\int ndt$ and T calculated from the fuel enthalpy, assuming a 2200-meter per second $U^{235}$ fission cross section of 582 barns, a Maxwellian thermal spectrum, an effective energy release of 173 Mev per fission, and a starting temperature of 20°C.

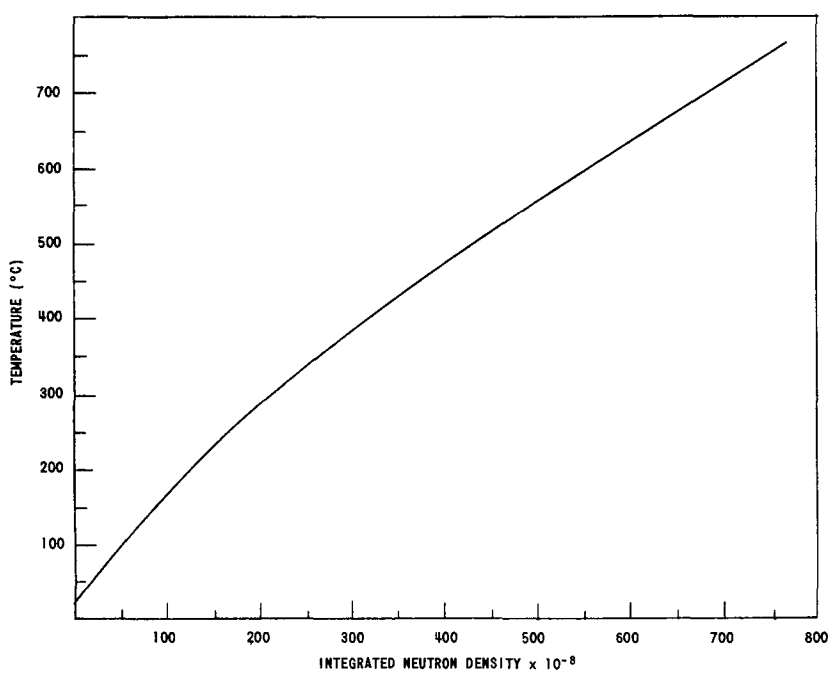


FIG. 23
TREAT TEMPERATURE - INTEGRATED NEUTRON DENSITY RELATIONSHIP

### 2. Calculations of $k_{ex}$ as a Function of $\int ndt$

Calculations of $k_{eff}$ as a function of T for a spherical TREAT-like system, using the 20-group cross sections and the "Fire" IBM-704 diffusion theory code, have been described in Section I. Those isothermal core results were converted to reactor $k_{ex}$ as a function of $\int ndt$, using the relationship of Fig. 23. Figure 24 shows the $k_{ex}$ vs. $\int ndt$ function thus derived, referred to $k_{ex} = 0$ at 20°C. For comparison, Fig. 24 also includes the $k_{ex}$ vs. $\int ndt$ relationship which is obtained using a constant temperature coefficient of reactivity:

$$\Delta k_{ex}/k_{eff} = -2.5 \times 10^{-4} \Delta T,$$

where T is in °C. In the work which follows, the shape of the curve obtained using the 20-group, gas model calculations is taken as appropriate in the absence of an adequate crystalline model treatment, but the absolute normalization is adjusted to fit experiment.

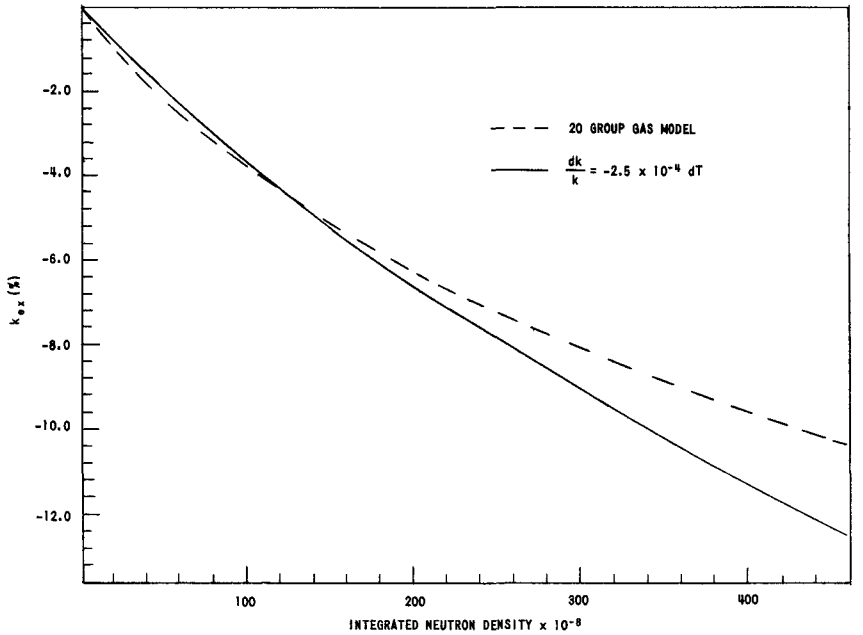


FIG. 24

CALCULATED $k_{ex}$ - INTEGRATED NEUTRON DENSITY RELATIONSHIP

## D. Fit to Experimental Data

### 1. Techniques

#### a. Theoretical Neutron Density Calculations

Such experimental results as maximum transient power, integrated transient power, maximum hot-spot temperature, and transient power curve shape were checked by comparison with kinetics calculations of neutron density.

The Argonne IBM-704 kinetics code RE-129* was used to calculate theoretical transients. It is the companion code to RE-171,[20] and provides values for n(t), given $k_{eff}$ as a function of time. The particular form of RE-129 used (129-H) permits $k_{eff}$ to be given as a function of time by the general form

$$k_{ex}(t) = k_{ex}(0) + \sum_i A_i t^i + \sum_i B_i \left[\int n dt\right]^i \quad , \tag{13}$$

where the $A_i$ and $B_i$ are constants, and i ranges from 1 to 4. The $A_i$ provide a convenient means for describing reactivity changes due to control rod motion, and the $B_i$ for describing a temperature coefficient of reactivity for a TREAT-like reactor. The code has provision for changing the values of the $A_i$ and $B_i$ at pre-set times. Thus, one may begin a theoretical transient describing rod motion with an input of reactivity given as a function of time by an arbitrary quartic equation. At a given time, corresponding to cessation of the rod movement, the $A_i$ are all set equal to zero.

b. Absolute Normalization of Theoretical Calculations

In order to compare the kinetics calculations of n(t) with experiment, it was necessary to normalize the calculations to experimental data. For the transients under study, the effects of the source are negligible, and the initial power levels are low enough that the reactor is essentially on its asymptotic period before heating produces appreciable reactivity changes. Hence, the shapes of calculated neutron-density curves should be independent of the absolute values of the power coefficient of $k_{ex}$, since $\dot{n}/n$ would be a function of $k_{ex}$ and be independent of n; that is, an n(t) calculation of such a transient using the RE-129H code may be scaled up or down in absolute magnitude as long as both n(t) and the $B_i$ are scaled together so that, at each point in the transient, the $k_{ex}$ change contributed by the $\sum_i B_i \left[\int n dt\right]^i$ remains unchanged. Hence, if n(t) be scaled according to $n(t) = C\, n(t)$, then the $B_i$ must be scaled as follows:

$$\sum_i B_i \left[\int n dt\right]^i = \sum_i B_i' \left[C^{-1} \int n dt\right]^i \quad , \tag{14}$$

where

$$B_i' = C^i B_i \tag{15}$$

Such a normalization of the $B_i$ is, of course, equivalent to multiplying the temperature coefficient of reactivity used (to calculate the $B_i$) by C.

* This is an IBM-704 version of the space-independent kinetics code RE 29 which was written for AVIDAC.[27]

Figure 25 illustrates this point. It shows the results of two RE-129H calculations of n(t) for identical values of $k_{ex}(0)$, the delayed-neutron parameters calculated for TREAT, a lifetime of $8.8 \times 10^{-4}$ sec, and the power coefficients of $k_{ex}$ differing only by a constant factor. For simplicity, all the $A_i$ and $B_i$ were taken as zero, except the two values of $B_1$; problem A was run with $B_1 = -2.50938 \times 10^{-12}$, and problem B with $B_1 = -5.01876 \times 10^{-12}$; $k_{ex}(0)$ was 1.1618%. For this simple case, then, the power ratio for corresponding points in the two transients, i.e., for maximum powers, one-half maximum powers, etc., is given by

$$\frac{\text{Power (Prob A)}}{\text{Power (Prob B)}} = \frac{B_1 \text{ (Prob B)}}{B_1 \text{ (Prob A)}} \quad . \tag{16}$$

In the somewhat more general case where the $A_i$ are still zero, but none of the $B_i$ are, this power ratio is not necessarily a constant throughout two different transients calculated with identical lifetimes, $k_{ex}(0)$, and delayed-neutron parameters. It will be a constant for two such problems if

$$\frac{B_i \text{ (Prob. 1)}}{B_i \text{ (Prob. 2)}} = C^i \quad , \tag{17}$$

where $C^i$ is the same for all i. Then the power ratio for corresponding points is

$$\frac{\text{Power (Prob. 2)}}{\text{Power (Prob. 1)}} = C \quad . \tag{18}$$

This inverse relation between power and power coefficient of $k_{ex}$ provides a means of normalizing the calculated power coefficient - and hence the temperature coefficient - to the experimental results for a given transient. Each $B_i$ is multiplied by $C^i$ as per Equation (15), where the C is given by the ratio of maximum power of the kinetics calculation to the maximum experimental power determined by averaging the maximum readings of the linear power instruments.

Normalizing calculation to experiment for the maximum power of the most severe transient ($k_{ex}(0) = 1.92\%$)* required a C of 0.88. This normalization was found to give a good and consistent fit to the experiments (see Section D-2), and was adopted as representing the reactor behavior. Table VIII summarizes the 20-group gas model results and normalization used for this fit.

---

*The initial $k_{ex}$ from the period measurement directly from the recorder was 1.90%.(9)

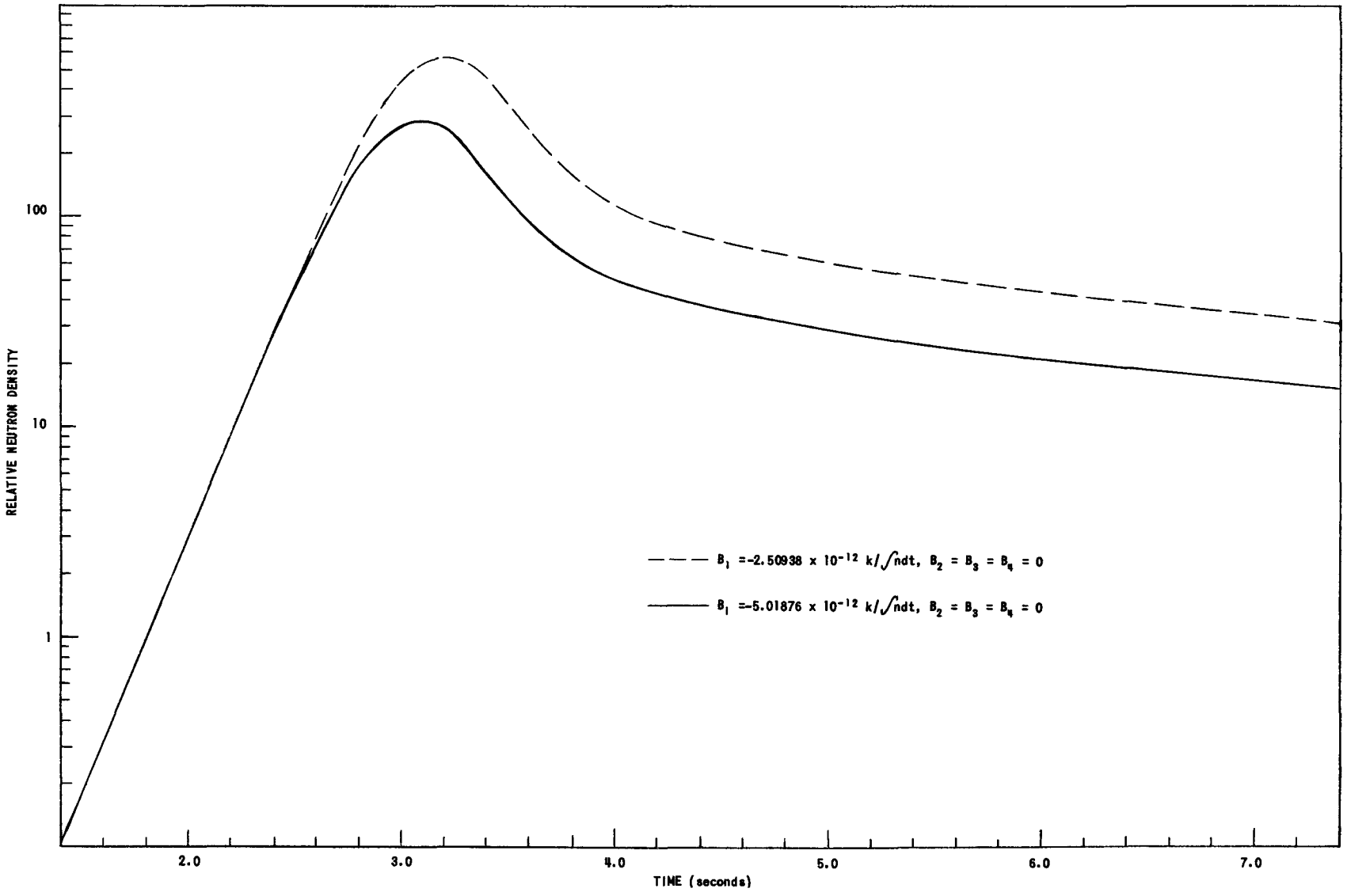


FIG. 25
POWER FEEDBACK NORMALIZATION EXAMPLE

Table VIII

NORMALIZATION OF 20-GROUP GAS MODEL CALCULATIONS

| Core Temperature T, °C | $k_{ex}(t)$, % | $\Delta k_{ex} = k_{ex}(t) - k_{ex}(27°C)$, % | Normalized $\Delta k_{ex}$, % |
|---|---|---|---|
| 27 | 2.833 | reference | problem |
| 127 | 0.081 | -2.75 | -2.42 |
| 227 | -2.289 | -5.12 | -4.50 |
| 327 | -4.295 | -7.13 | -6.27 |
| 477 | -6.824 | -9.66 | -8.49 |
| 627 | -8.961 | -11.79 | -10.38 |

This normalization is independent of the values chosen for the fission cross section and the energy release per fission, since the same values were used in converting from measured power to experimental neutron density, and from temperature coefficient of feedback to the $B_i$.

c. Check of Feedback Curve Shape

In principle, one may obtain the simplest and most direct check on the power coefficient of reactivity by comparing theory directly against the values of $k_{ex}(t) - k(0)$ as a function of $\int n dt$ for the ensemble of experiments studied. Early in the analysis, however, it was found that scatter in the data derived from transient experiments was sufficient to make such a comparison a rather insensitive one for checking either the absolute magnitude of the feedback relations or the shape of the power coefficient of reactivity curve.

Both the absolute magnitude and shape of the feedback relationship can be checked by comparing experimental and calculated values of maximum power. However, this technique is limited to checking the feedback for $k_{ex}$ changes equal to those occurring between initiation of the transients and peak transient power. Since $k_{ex}$ at the peak is $\sim\beta$ for super-prompt-critical excursions and the maximum $k_{ex}(0)$ used was 1.92%, the check of peak powers was a check on feedback only up to a $k_{ex}$ change of $\sim 1.92 - 0.72 = 1.2\%$.

A testing of the shape of the feedback curve to higher temperatures can be obtained by comparing the shapes of experimental and calculated neutron-density curves beyond the peak. For this purpose, three

calculations were run for each of three experimental transients ($k_{ex}(0)$ of 0.595%, 1.16%, and 1.92%, respectively). One calculation was made using the 20-group gas model temperature feedback results. One was made using the $B_i$ calculated under the assumption of a constant temperature coefficient of reactivity. And one was made for the assumption of a constant power coefficient of reactivity ($B_2=B_3=B_4=0$), which differs from the constant temperature coefficient case because of the nonconstancy of specific heat.

As an additional test of the normalized 20-group gas model feedback, a theoretical transient was compared with the experimental results of Transient 17. This was a transient initiated by 0.69% $k_{ex}$ with elevated starting core temperatures which, if averaged over the core, would be equivalent to a uniform temperature of 82°C.

2. Results of Comparisons

a. Direct Comparison of Calculated and Experimental Feedback

As noted previously, the feedback data derived from experiment were used only for orientation purposes because the scatter in these data precluded their use for any detailed check against calculation. Values of integrated power as a function of time for each transient were obtained by integrating the reactor power from the instrument readings to the time of peak power, and (depending on the range of data available) to one, two, or three points beyond. These numbers were converted to values of integrated neutron density using Equation (12). The change in $k_{ex}$ due to each of the values of $\int ndt$ was taken from the $k_{ex}$ calculations made using RE-171, in conjunction with the power instrument readings.

A small correction was made to adjust the data to a uniform starting temperature of 20°C in the following manner. The relationship between changes in $k_{ex}$ and changes in integrated neutron density was estimated from the data. An integrated neutron density which would raise the fuel from 20°C to the starting temperature of a given transient was derived and added to the values calculated from the instrument records of that transient. Similarly, an increment in $k_{ex}$ corresponding to the rise in temperature from 20°C to the starting temperature was calculated and added to the changes in $k_{ex}$.

These data, for all the experimental transients, are graphed in Fig. 26, and provide an empirical relation between $k_{ex}$ and $\int ndt$. Three theoretical curves are included for comparison: one based on the temperature-reactivity relation from the 20-group gas model calculations, one assuming a constant temperature coefficient of $\Delta k_{ex}/k_{eff} = -2.5 \times 10^{-4}\ \Delta T$, and one based on the normalized 20-group gas model results that were finally adopted.

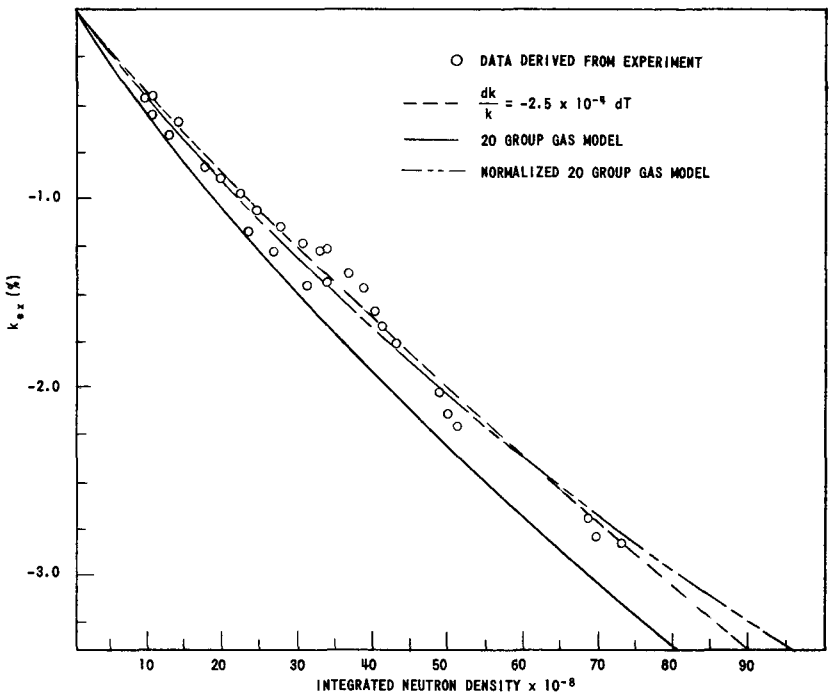


FIG. 26

COMPARISON OF CALCULATED AND EXPERIMENTAL $k_{ex}$ - INTEGRATED NEUTRON DENSITY DATA

b. Power Curve Shapes

The results of comparison of calculated and experimental power curve shapes are given in Figs. 27, 28, 29 and 30, which show the log 1 power records of transients initiated with $k_{ex}$ of 0.595%, 1.16% and 1.92%, respectively. A log power instrument was chosen for the figures to demonstrate the degree of agreement over as wide a power range as possible. Each of the three figures also includes the theoretical power curves for: (1) a feedback shape given by the 20-group gas model calculations; (2) a constant temperature coefficient of reactivity; and (3) a constant power coefficient of reactivity.

Figure 30 shows the log 1 power record and theoretical results using the normalized 20-group gas model feedback for transient 17, the elevated-temperature 0.69% $k_{ex}$ excursion.

For purposes of comparison in the four figures, the maximum power of each calculation was normalized to the maximum power of the corresponding experimental transient. The comparisons demonstrate that the detailed shape of the feedback relation is relatively unimportant for the sub-prompt-critical transients, since all three feedback curves are relatively straight over this narrow range of $k_{ex}$ change, but becomes increasingly more important as $k_{ex}(0)$ becomes greater than $\beta_{eff}$. It is seen that the fit of the feedback derived from the 20-group gas model calculations is quite satisfactory.

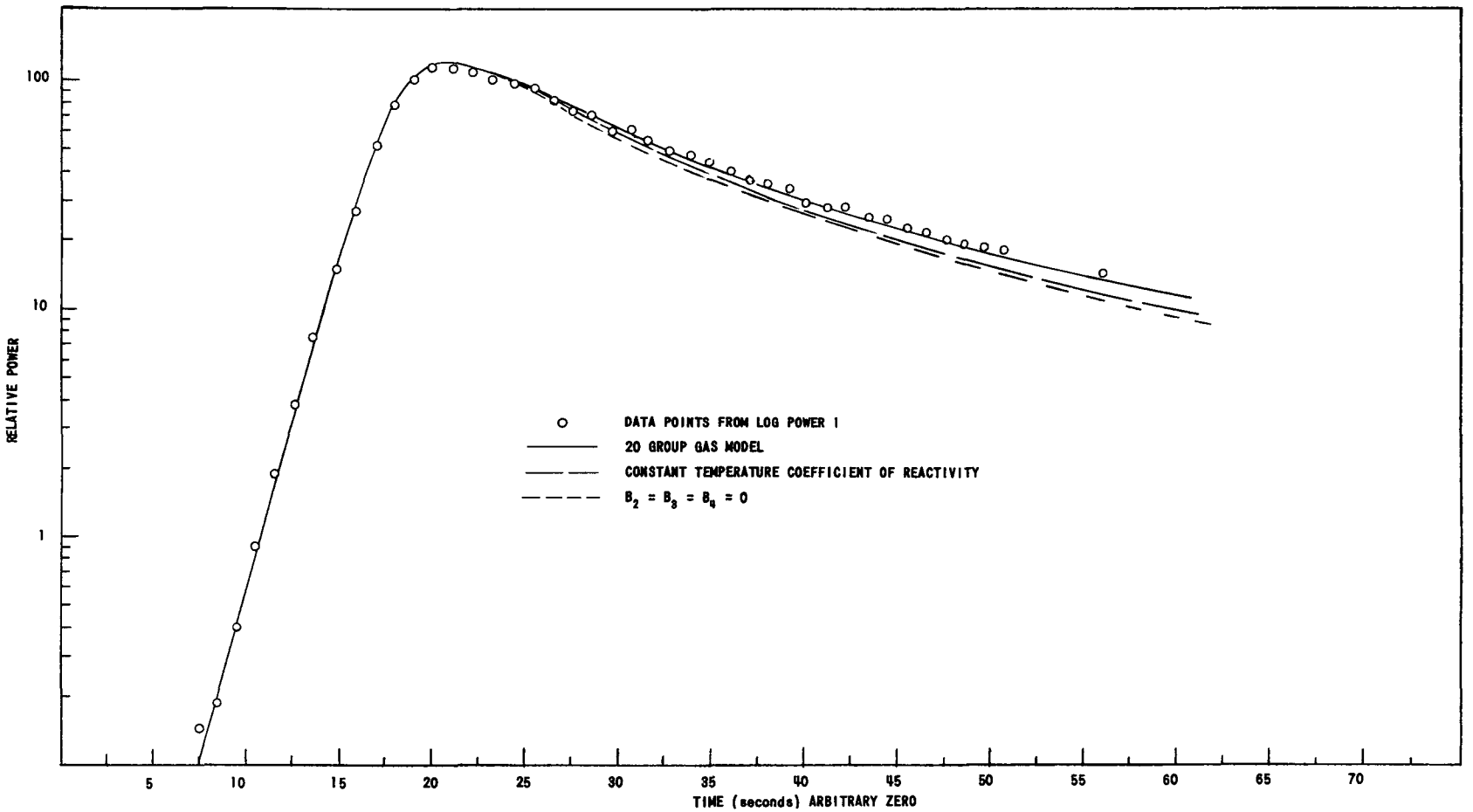


FIG. 27
COMPARISON OF CALCULATED AND EXPERIMENTAL POWER CURVE SHAPES
FOR 0.595% $k_{ex}$ TRANSIENT

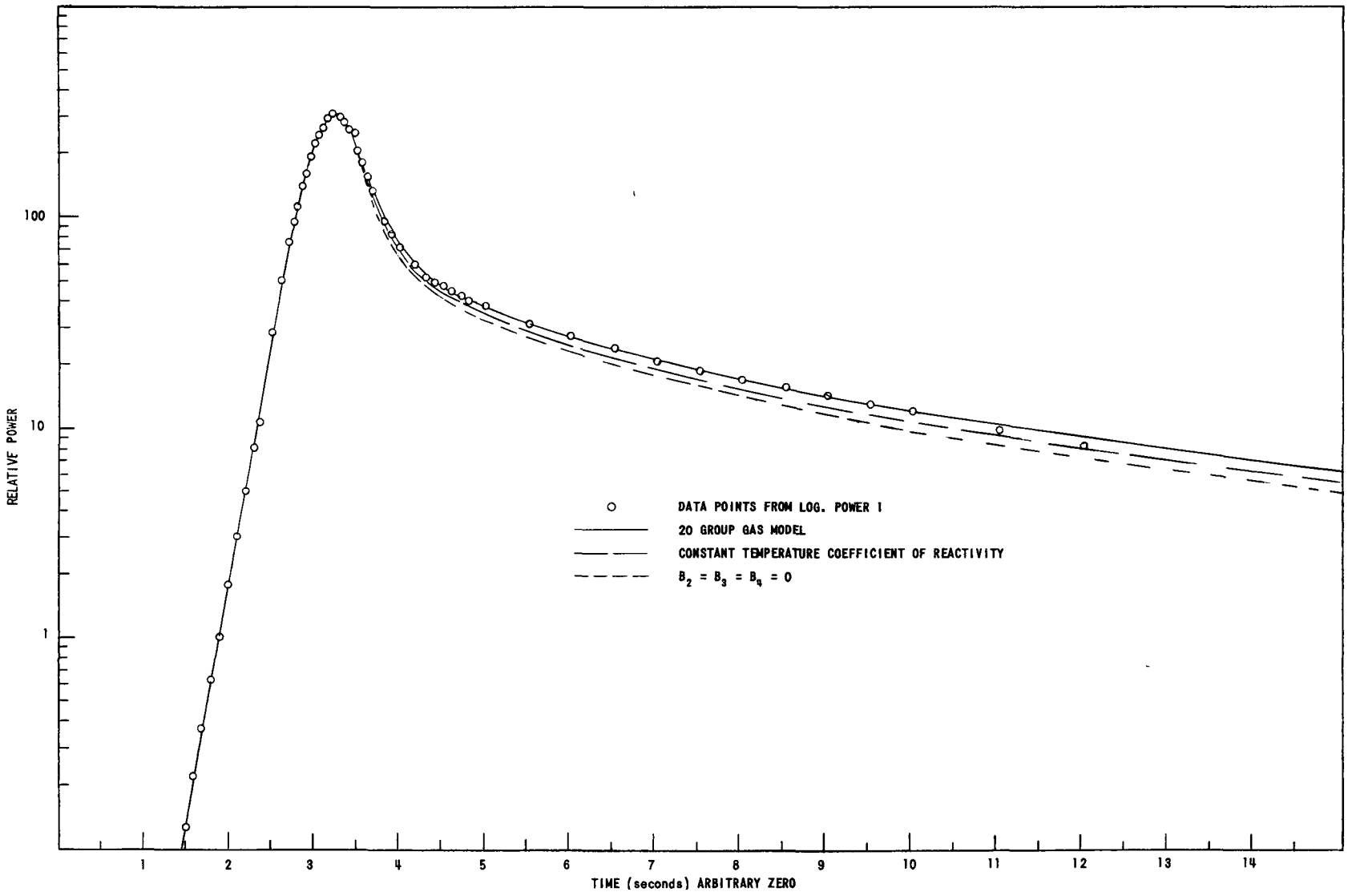


FIG. 28

COMPARISON OF CALCULATED AND EXPERIMENTAL POWER CURVE SHAPES FOR 1.16% $k_{ex}$ TRANSIENT

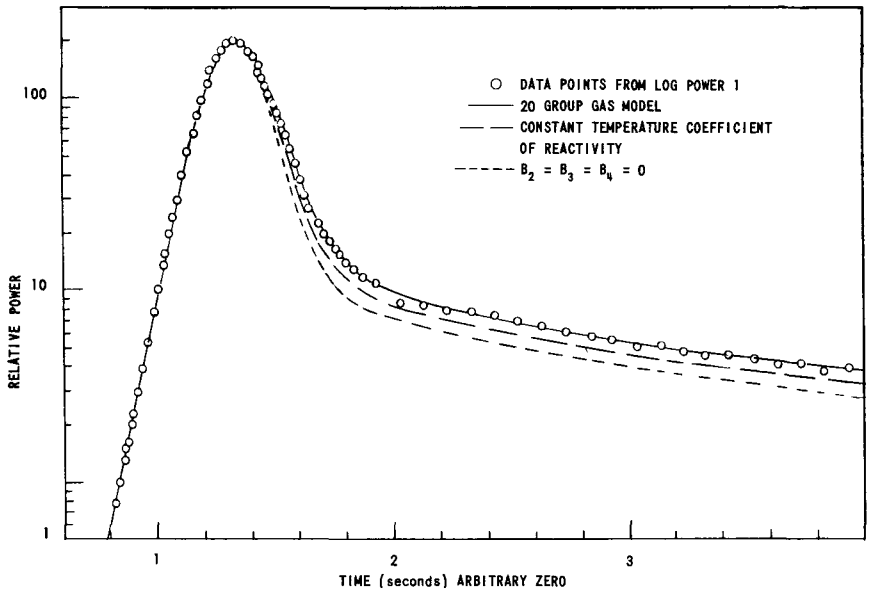


FIG. 29
COMPARISON OF CALCULATED AND EXPERIMENTAL POWER CURVE SHAPES FOR 1.92 $K_{ex}$ TRANSIENT

c. Maximum Transient Power Values

Experimental values of peak power, as determined by an averaging of the two linear instruments, are plotted in Fig. 31 as a function of initial $k_{ex}$, as calculated from the reactor period data. Three theoretical curves are shown with the data: one for the feedback relation given by the 20-group gas model calculations; one for a constant temperature coefficient of reactivity given by $\Delta k_{ex}/k_{eff} = -2.5 \times 10^{-4}\ \Delta T$; and one for the 20-group gas model feedback normalized to the peak power of the transient initiated with 1.92% $k_{ex}$ (as described in Section II-D). The last relation does provide the best description of the three shown.

The point for Transient 17 falls appreciably off the theoretical curve, because of the elevated starting temperatures. The experimental value of 15.8 Mw may be compared with a calculated value of 14.4 Mw.

d. Integrated Power Values

Another comparison between calculation and experiment is given in Fig. 32, which shows the integrated power calculations, obtained with the RE-129H code using the normalized 20-group gas model feedback, and experimental values of integrated power graphed as a function of initial $k_{ex}$. All the theoretical transients were initiated with a step function input of $k_{ex}$ at a power level of 10 watts and run to a final time of 60 sec.

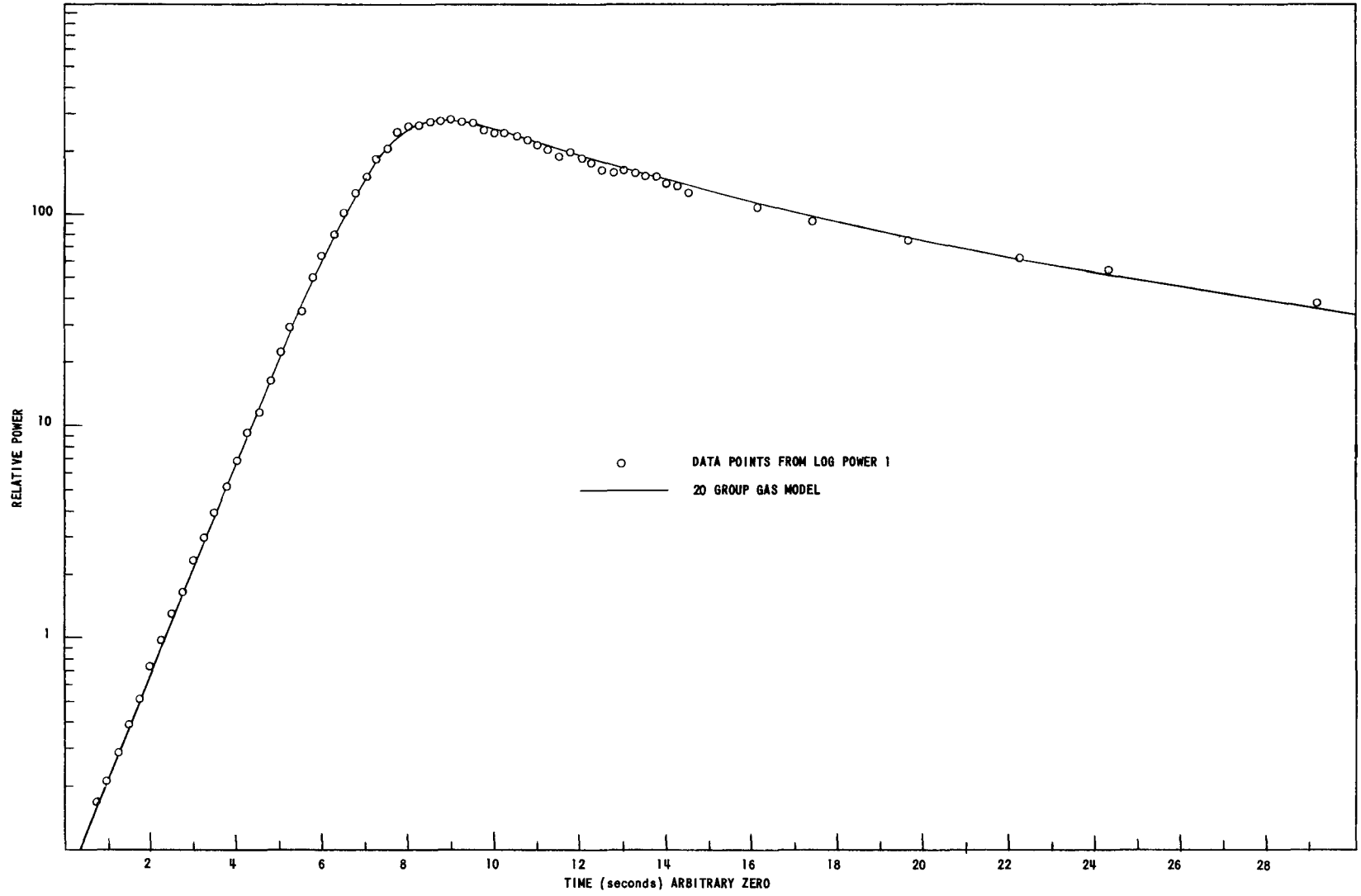


FIG. 30
COMPARISON OF CALCULATED AND EXPERIMENTAL POWER CURVE SHAPES
FOR THE TRANSIENT INITIATED AT ELEVATED TEMPERATURE

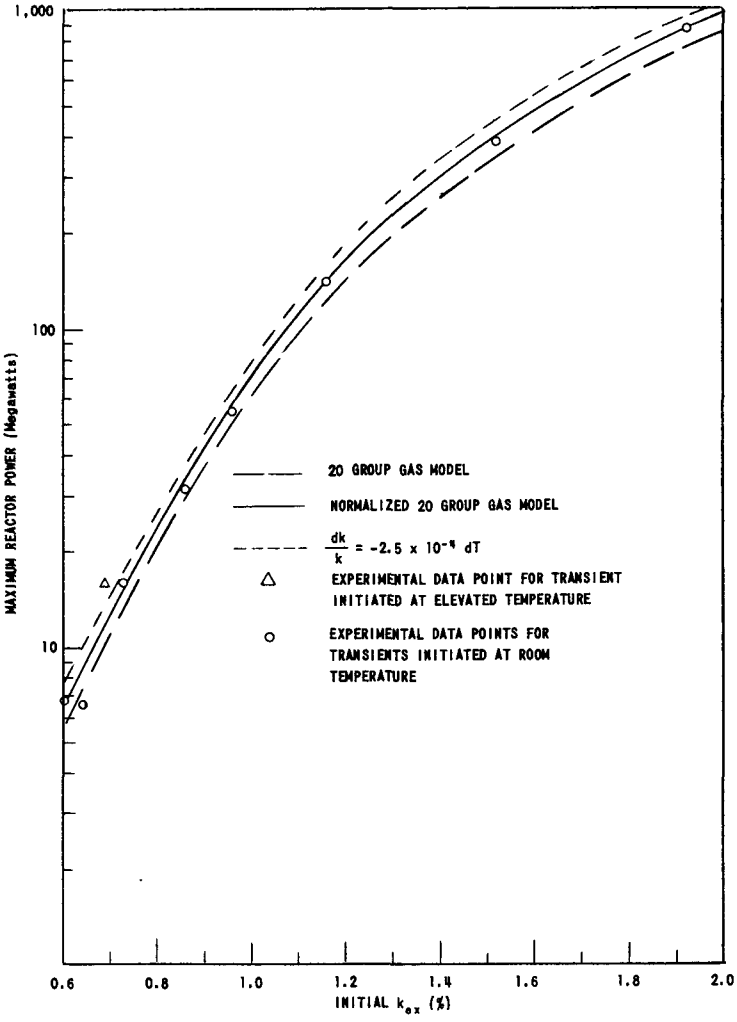


FIG. 31

COMPARISON OF CALCULATED AND EXPERIMENTAL MAXIMUM TRANSIENT POWER DATA

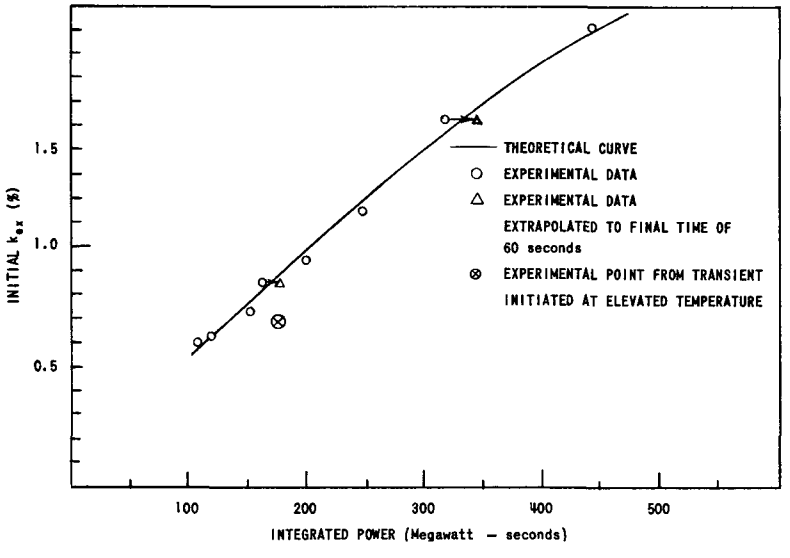


FIG. 32

COMPARISON OF CALCULATED AND EXPERIMENTAL INTEGRATED TRANSIENT POWER DATA

This final time was chosen because, for the majority of the transients, the change in integrated power as a function of time is essentially negligible at 60 sec. The "lonely" point of 172 Mw-sec from Transient 17 is included on the graph for completeness. A calculation, by means of the normalized 20-group gas model feedback, of the integrated power from a 0.69% transient begun at the actual starting core temperatures of Transient 17 yielded a value of 171 Mw-sec.

A correction was made for the estimated 9 Mev/fission of decay energy released during the 60-sec duration of a burst. The conversion factor, calculated using 173 Mev/fission, represents the instantaneous energy absorption, and the computer integrated power results were multiplied by 182/173 to account for the decay energy.

Also included in Fig. 32 are the experimental integrated power data obtained from the two fission counters in the reactor shielding. Nearly all of the transients were clipped at times between 50 and 60 sec and the data were corrected to a uniform final time of 60 sec. The corrections are small for all transients except two, which were clipped at less than 30 sec. These two are indicated as extrapolations on the figure. Values of initial $k_{ex}$ for the experimental points were calculated from the asymptotic transient periods.

e. Maximum Reactor Temperatures

Given the calculated values of integrated power, it is possible to derive maximum reactor temperatures. Since the reactor kinetics calculations are space-independent, they yield only integrated power values corresponding to average core temperature rises. Multigroup reactor calculations (see Section I) had indicated for TREAT a maximum-to-average neutron density ratio of about 1.62. However, numerical integration of the foil and counter measurements yielded a ratio of 1.71.[9] Accordingly, the theoretical integrated neutron density at the point of maximum neutron density was obtained by multiplying the core-averaged integrated neutron density from the RE-129H calculations, corrected for the decay energy, by 1.71. The temperature rise corresponding to this maximum neutron density was then calculated using the fuel enthalpy data.

Figure 33 shows the theoretical maximum core temperatures as a function of initial $k_{ex}$, calculated assuming an initial uniform core temperature of 30°C and power integrated to a final time of 60 sec. Also included are the experimental maximum temperatures, based on readings from the thermocouple nearest to the point of maximum neutron density. The experimental data are corrected to a uniform starting temperature of 30°C, a final time of 60 sec, and for the difference between the maximum core neutron density and the density at the thermocouple position.

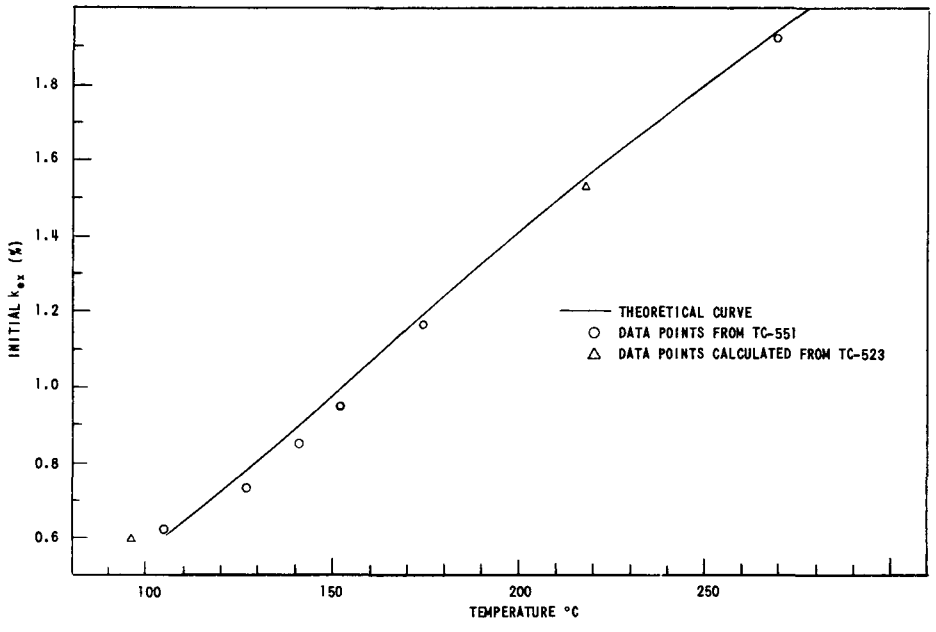


FIG. 33
COMPARISON OF CALCULATED AND EXPERIMENTAL MAXIMUM REACTOR TEMPERATURE DATA

## E. Performance Extrapolations

Because of the success achieved in using the normalized 20-group gas model feedback to describe TREAT transient behavior, the fuel enthalpy data were combined with the full temperature range covered by the 20-group gas model calculations (see Fig. 24) to yield $B_i$ for kinetics calculations of neutron density and integrated neutron density over a much wider temperature range than covered in the experiments. The $B_i$ were normalized to experiment, as before, using C = 0.88.

Figure 34 shows the extended calculation of normalized $k_{ex}$ corresponding to $\tau$, for a starting temperature of 20°C. Figure 35 gives the theoretical power curves of transients initiated at 30°C with $k_{ex}$ of 2.5%, 3.2%, 4.4% and 5.6%. Figure 36 shows reactor integrated power as a function of initial $k_{ex}$, assuming a starting temperature of 30°C, a final time of 60 sec, and the 5.2% decay correction. Figure 37 gives the theoretical values of maximum reactor temperature, assuming a starting temperature of 30°C, a final time of 60 sec, a reactor maximum-to-average neutron density ratio of 1.7, and the decay correction. Figure 38 shows the peak power as a function of initial $k_{ex}$ for transients started at 30°C.

The predictions indicate that a 2.97% $k_{ex}$ transient initiated at 30°C would result in a maximum core temperature of 400°C, a peak power of 3900 Mw, and an integrated power of 950 Mw-sec. This estimate applies to the simplest reactor geometry. With the insertions of an experiment and of large viewing slots into the core, perturbations in the flux and increases in core size modify this estimate somewhat.

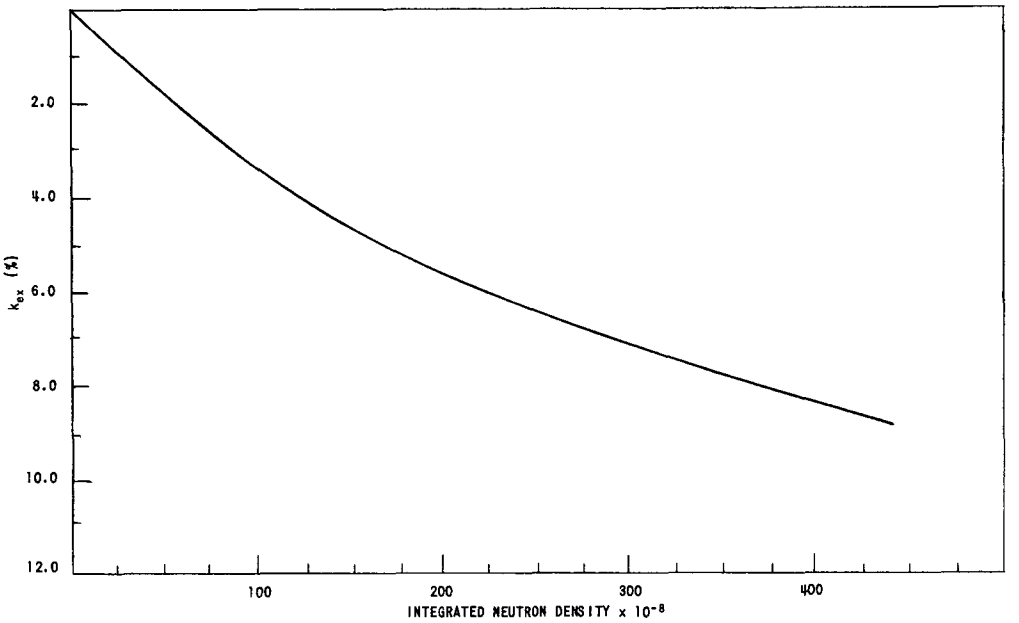


FIG. 34

TREAT EXTRAPOLATED NORMALIZED $k_{ex}$ — INTEGRATED NEUTRON DENSITY RELATIONSHIP

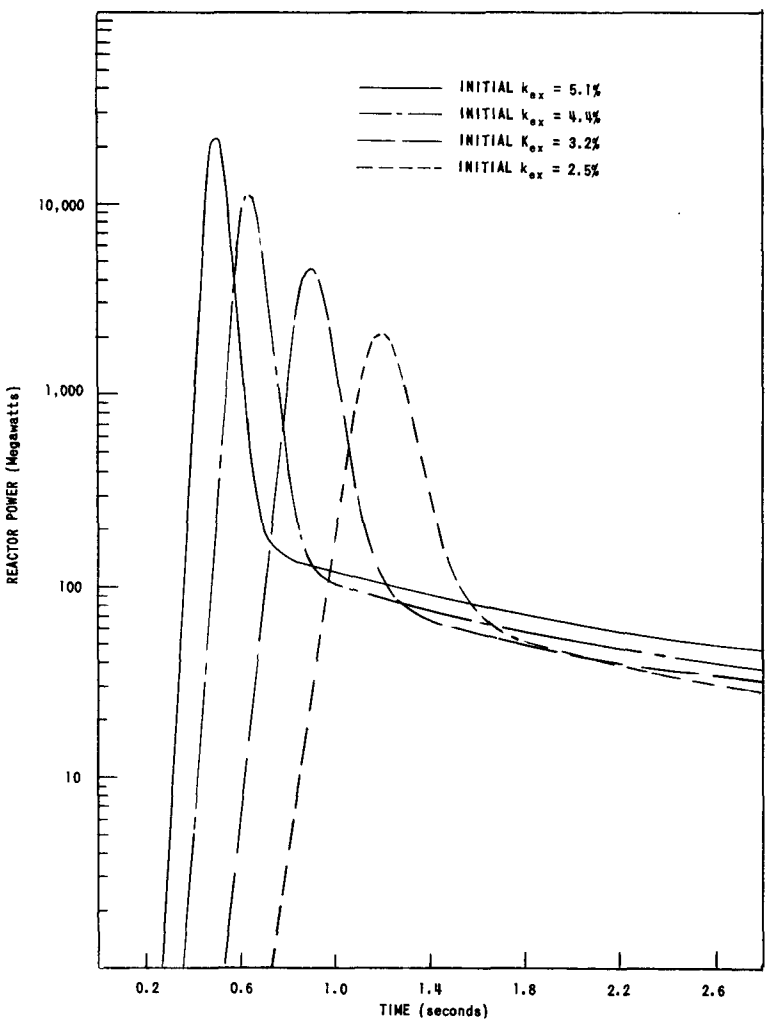


FIG. 35

TRANSIENT POWER CURVES CALCULATED USING EXTRAPOLATED NORMALIZED FEEDBACK

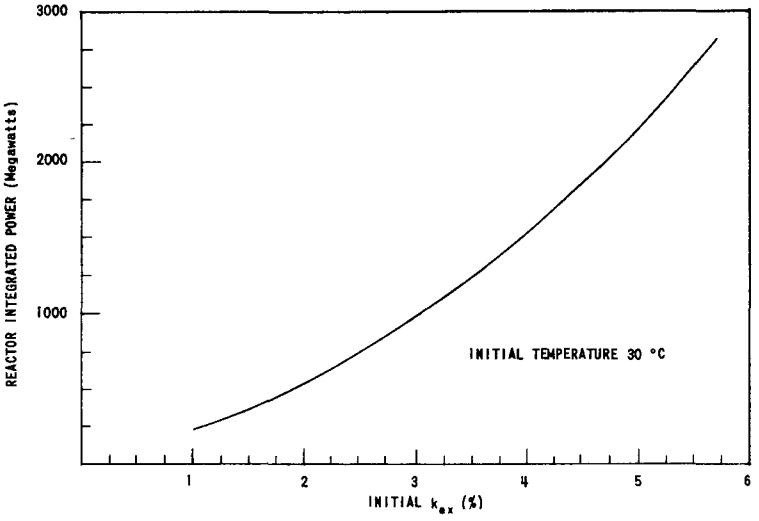


FIG. 36
INTEGRATED TRANSIENT POWER VALUES CALCULATED
USING EXTRAPOLATED NORMALIZED FEEDBACK

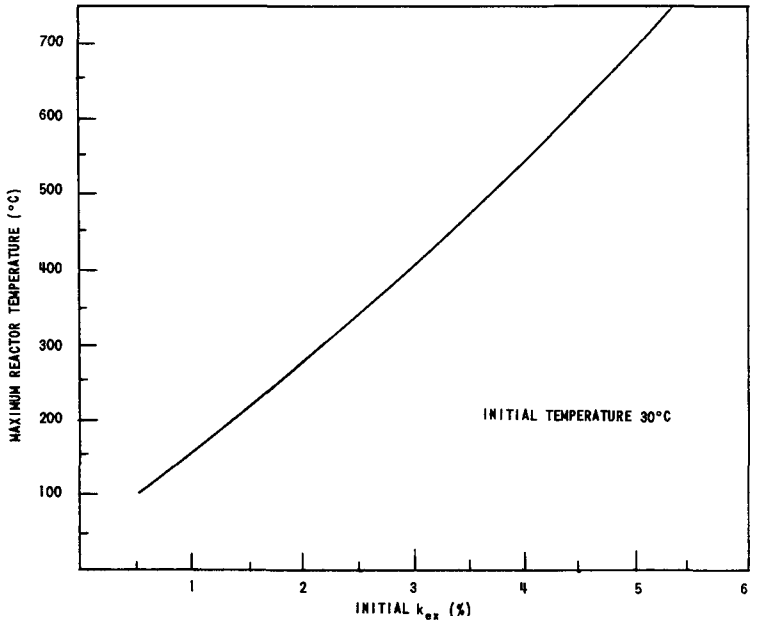


FIG. 37
MAXIMUM REACTOR TEMPERATURES CALCULATED
USING EXTRAPOLATED NORMALIZED FEEDBACK

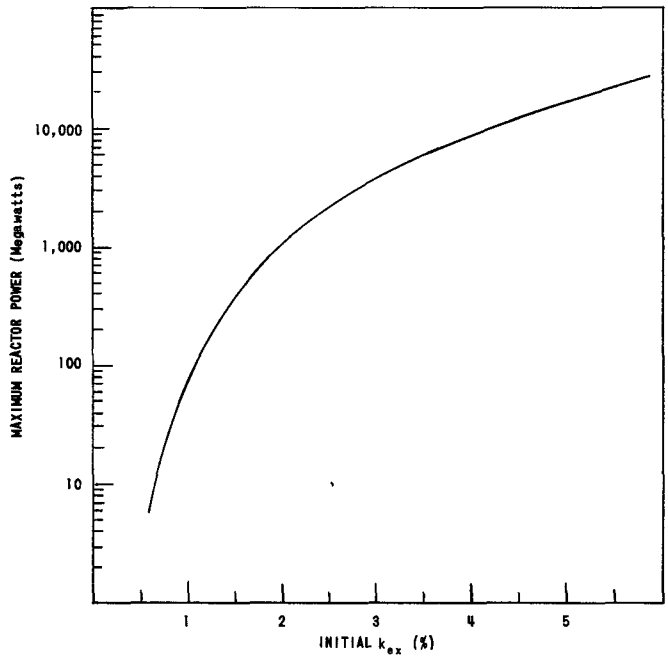


FIG. 38
MAXIMUM TRANSIENT POWER VALUES CALCULATED
USING EXTRAPOLATED NORMALIZED FEEDBACK

Corrosion measurements have demonstrated that the Zircaloy cladding of the TREAT fuel should have a life of the order of years under continuous operation at 400°C.[3] Probably 700°C is the limiting temperature for short time operation.[3] The extended-range calculations predict that 700°C would be the maximum core temperature attained for a transient initiated at 30°C with 5.05% $k_{ex}$. The integrated power of such a transient would be 2260 Mw-sec, and the peak power would be 17,000 Mw.

## REFERENCES


1. W. J. McCarthy, Jr., R. B. Nicholson, D. Okrent, and V. Z. Jankus, Studies of Nuclear Accidents in Fast Power Reactors, Proceedings of the Second United Nations International Conference on the Peaceful Uses of Atomic Energy, Geneva, Vol. 12, 207 (1958).

2. G. A. Freund, H. P. Iskenderian, and D. Okrent, TREAT, A Pulsed Graphite-moderated Reactor for Kinetic Experiments, Proceedings of the Second International Conference on the Peaceful Uses of Atomic Energy, Geneva, Vol. 10, 461 (1958).

3. D. R. MacFarlane, G. A. Freund, and J. F. Boland, Hazards Summary Report on TREAT, ANL-5923 (1958).

4. G. A. Freund, P. Elias, D. R. MacFarlane, J. D. Geier, and J. F. Boland, Design Summary Report on the Transient Reactor Test Facility (TREAT), ANL-6034 (June 1960).

5. H. P. Iskenderian, Physics Analysis of the TREAT Reactor Design, ANL-6025 (1959).

6. H. P. Iskenderian, Post Criticality Studies on the TREAT Reactor, ANL-6115 (1960).

7. J. F. Boland, F. Kirn, and D. Okrent, The Kinetics of TREAT. I. Experimental Results and Their Correlation, Trans. ANS, 2 (2) 54 (1959).

8. D. Okrent, D. F. Schoeberle, and L. Lois, The Kinetics of TREAT. II. Comparison of Experiment and Theory, Trans. ANS, 2 (2) 55 (1959).

9. F. Kirn, J. F. Boland, R. D. Cook, and H. Lawroski, Reactor Physics Measurements in TREAT, ANL-6173 (to be published).

10. J. Handwerk, Private Communication.

11. J. E. Hill, L. D. Roberts, and G. McCammon, The Slowing Down of Fission Neutrons in Graphite, AECD-3390 (1940) or ORNL-187 (1949).

12. E. R. Cohen, The Neutron Velocity Spectrum in a Heavy Moderator, Nuc. Sci. Eng. 2, 227 (1957), or NAA-SR-1940 (October 1957).

13. E. H. Bareiss, J. E. Denes, and V. Z. Jankus, Calculation of Group Cross Sections for Hot Monatomic Moderator with Variable Flux Weighting Within Groups, ANL-5984 (1959).

14. H. Hurwitz, Jr., M. S. Nelkin, and G. J. Habetler, Neutron Thermalization. I. Heavy Gaseous Moderator, Nuc. Sci. Eng. 1, 280 (1956).

15. R. B. Tattersall, H. Rose, S. K. Pattenden, and D. Jowitt, Pile Oscillator Measurements of Resonance Absorption Integrals, A.E.R.E.-R. 2887 (1959).

16. Reactor Physics Constants, ANL-5800 (1958).

17. F. Brinkley, A One-dimensional Intermediate Reactor Computing Program, LA-2161 (Supplement) (1960).

18. D. Meneghetti and K. E. Phillips, Calculation of the Temperature Dependence of $Pu^{239}/U^{235}$ Fission Ratio for a Graphite-$U^{235}$ System, ANL-6058 (1959).

19. W. P. Stinson, L. C. Schmid, and R. E. Heineman, An Investigation of Effective Neutron Temperatures, Nuc. Sci. Eng. 7, 435 (1960).

20. I. G. Baksys (Private Communication).

21. M. Butler (Private Communication).

22. G. R. Keepin, T. F. Wimett, and R. K. Zeigler, Delayed Neutrons from Fissionable Isotopes of Uranium, Plutonium, and Thorium, J. Nuc. Energy 6, No. 1/2, 1-21 (1957).

23. R. Gwin, Determination of Reactor Parameters from Period Measurements, Applied Nuclear Physics Annual Report, ORNL-2081 (September 1956).

24. A. M. Weinberg and E. P. Wigner, The Physical Theory of Neutron Chain Reactors (Chicago: The University of Chicago Press, 1958).

25. G. R. Keepin, T. F. Wimett, and R. K. Zeigler, Delayed Neutrons from Fissionable Isotopes of Uranium, Plutonium, and Thorium, Phys. Rev. 107, 1044 (1957).

26. H. W. Beam (Private Communication to J. H. Handwerk).

27. R. O. Brittan, Some Problems on the Safety of Fast Reactors, ANL-5577 (1956).